Degree Project in Electrical Engineering

Second cycle, 30 credits

Harmonic Backscattering for Zero-Energy Devices

Mathematical modeling and performance assessment

PASCHALINA FOTI

Harmonic Backscattering for Zero-Energy Devices

Mathematical modeling and performance assessment

PASCHALINA FOTI

Master's Programme, Communication Systems, 120 credits
Date: December 06, 2024

Supervisors: Mahmoud Zaher, Boules Nessim, Thiemo Voigt
Examiner: Emil Björnson
School of Electrical Engineering and Computer Science
Host company: Ericsson AB
Swedish title: Harmonisk bakåtspridning för nollenergienheter
Swedish subtitle: Matematisk modellering och prestandautvärdering

Abstract

The rise of Internet of Things (IoT) devices and advancements in the beyond 5G and 6G networks field have imposed the need for innovative low-power communication methods. Backscattering communication offers a promising solution for energy-efficient operation of Zero-Energy Devices (ZEDs). By reflecting incident signals instead of generating their own carrier, these devices communicate with minimal energy consumption, making them suitable for widespread deployment. A major challenge in backscattering is managing self-interference, where the external carrier signal interferes with the backscattered signal at the receiver, especially in monostatic setups.

Harmonic backscattering is proposed to address this issue by shifting the backscattered signal to a harmonic frequency, isolating it from the carrier, thereby eliminating self-interference. However, its modeling and effectiveness compared to traditional backscattering have not been thoroughly investigated.

This thesis develops a mathematical model for harmonic backscattering and evaluates its performance in terms of Bit Error Ratio (BER) vs Signal-to-Noise Ratio (SNR), comparing it with regular backscattering in both monostatic and bistatic setups.

The study employs theoretical modeling and simulations to assess various scenarios of interference and noise conditions. The results indicate that harmonic backscattering outperforms regular backscattering, especially in high-interference environments, by improving the BER performance for a given SNR value.

The findings of the thesis are of great significance for enhancing backscatter communication systems in IoT. By mitigating self-interference, harmonic backscattering enables more reliable ZED communication, supporting future innovations and advancements in IoT technology, while contributing to sustainable development by reducing the power consumption of IoT devices.

Keywords

Backscattering communication, Orthogonal Frequency Division Multiplexing, IoT, Low-power communication, 6G

Sammanfattning

Ökningen av IoT-enheter och framsteg inom området har skapat ett behov av innovativa lågströmskommunikationsmetoder. Bakåtspridningskommunikation erbjuder en lovande lösning för energieffektiv drift av ZED-enheter. Genom att reflektera befintliga signaler istället för att generera nya, kommunicerar dessa enheter med minimal energiförbrukning, vilket gör dem lämpliga för omfattande användning. En stor utmaning inom bakåtspridningskommunikation är att hantera självintrång, där den reflekterade signalen kan störa den ursprungliga bärarsignalen, särskilt i monostatiska uppsättningar.

Harmonisk bakåtspridning föreslås som en lösning på detta problem genom att flytta den reflekterade signalen till en harmonisk frekvens, vilket isolerar den från bäraren och därmed eliminerar självintrång. Dock har dess modellering och effektivitet jämfört med traditionell bakåtspridning inte undersökts grundligt.

Denna avhandling utvecklar en matematisk modell för harmonisk bakåtspridning och utvärderar dess prestanda i termer av BER mot SNR, och jämför den med vanlig bakåtspridning i både monostatiska och bistatiska uppsättningar.

Studien använder teoretisk modellering och simuleringar för att bedöma olika scenarier av störningar och brusförhållanden. Resultaten visar att harmonisk bakåtspridning överträffar vanlig bakåtspridning, särskilt i miljöer med hög störning, genom att erbjuda en renare signal med lägre BER.

Avhandlingens resultat är av stor betydelse för att förbättra bakåtspridningskommunikationssystem inom IoT. Genom att minska självinterferens möjliggör harmonisk backscattering mer tillförlitlig ZED-kommunikation, vilket stödjer framtida innovationer och framsteg inom IoT-teknologi, samtidigt som det bidrar till hållbar utveckling genom att minska energiförbrukningen hos IoT-enheter.

Nyckelord

Bakåtspridningskommunikation, Ortogonal frekvensdelningsmultiplexering, IoT, Lågströmskommunikation, 6G

Acknowledgments

I would like to express my deepest gratitude to my host company, Ericsson, for providing me with the opportunity to conduct this project. Their support and resources were invaluable to the success of my thesis.

I am grateful to my examiner, Emil Björnson, for his constructive feedback and support. His insights greatly enhanced the quality of my work. My heartfelt thanks also go to my university supervisor, Mahmoud Zaher, for his continuous support and guidance, both in the technical aspects and the planning of this thesis.

A special thank you goes to my primary supervisor, Boules Nessim, for his exceptional support, and constructive feedback, and for inspiring me with engaging ideas and conversations. His patience throughout my learning process was greatly appreciated. I would also like to thank my second supervisor, Thiemo Voigt, for the stimulating discussions and for providing diverse perspectives into solving occurring problems. Additionally, I am greatly thankful to Mehrnaz Afshang for her remote supervision, constructive feedback, and her expertise on the topic.

I extend my gratitude to my manager, Per Bjuréus, for the opportunity and assistance at the company, and to everyone at the S&T team for making me feel like a part of the group. I had an amazing time conducting my thesis at Ericsson. Special thanks to Hasti for being the best thesis buddy.

Lastly, I would like to thank my parents for their unwavering support and encouragement in all my endeavors. To my friends Mar, Rasmus, Amaury, Ferran, Fabi, Jonathan, Antonio, Wenjian, Chris, and Mayte thank you for sharing unforgettable experiences and making Stockholm feel like home. To my friends back in Greece, Anthie, Chara, Eleni, and Stefania, thank you for reminding me of home and sharing my journey abroad with me.

Stockholm, December 2024
Paschalina Foti

Contents

List of Figures

List of Tables

List of acronyms and abbreviations

ADC	Analog-to-Digital Converter
AI	Artificial Intelligence
AIoT	Ambient Internet of Things
ASK	Amplitude Shift Keying
AWGN	Additive White Gaussian Noise
BD	Backscatter Device
BER	Bit Error Ratio
BFSK	Binary Frequency Shift Keying
BLE	Bluetooth Low Energy
BPF	Bandpass Filter
BPSK	Binary Phase Shift Keying
CE	Carrier Emitter
CIR	Carrier-to-Interference Ratio
CLS	Carrier Leakage Suppression
CPFSK	Continuous-Phase FSK
CW	Carrier Wave
DL	Downlink
FDD	Frequency Division Duplex
FFT	Fast Fourier Transform
FSK	Frequency Shift Keying
IFFT	Inverse Fast Fourier Transform
IM	Intermodulation
IoT	Internet of Things
MSK	Minimum Shift Keying
OFDM	Orthogonal Frequency-Division Multiplexing
OOK	On-Off Keying
PAPR	Peak-to-average Power Ratio
PDF	Probability Density Function

PMU	Power Management Unit
PSK	Phase Shift Keying
RD	Reader
RF	Radio Frequency
RFID	Radio Frequency Identification
SIR	Signal-to-Interference Ratio
SNR	Signal-to-Noise Ratio
SWIPT	Simultaneous Wireless Information and Power Transfer
UE	User Equipment
UHF	Ultra High Frequency
UL	Uplink
WISP	Wireless Identification and Sensing Platform
WPT	Wireless Power Transfer
WSN	Wireless Sensor Network
ZE	Zero-Energy
ZED	Zero-Energy Device

Chapter 1

Introduction

In today's interconnected world, wireless communication plays a crucial role in shaping modern society. At the forefront of this technological revolution are the advancements in cellular networks, particularly the transition from 4G to 5G, which has improved the speed and reliability of wireless networks, and has paved the way for seamless integration of the Internet of Things (IoT) into various industry sectors. With 14.3 billion global active IoT connections in 2022 and an estimated 29.7 billion connections projected to be active by 2027 [1], IoT connectivity is not only transforming industries but also fostering substantial economic growth. From a business perspective, the IoT market is highly competitive with an expected revenue of more than 1 trillion US$ in 2024 [2].

One of the key technologies in IoT connectivity is cellular IoT, which currently makes up nearly 20% of the global IoT connections [1, 3]. With 6G on the horizon, the emergence of low-power communication protocols and Zero-Energy Devices (ZEDs) represents a shift towards sustainable technology. Together, these developments define the landscape of wireless communication, influencing how we connect, communicate, and interact with the world.

In this thesis, we will examine the use of ZEDs in cellular networks and investigate ways in which the performance of such systems can be improved. The focus is on the area of wireless communications and energy harvesting technologies. More specifically, the scope of the project is to enhance backscattering communication for ZEDs, by studying and implementing advanced interference avoidance techniques and particularly focusing on harmonic backscattering.

1.1 Background

The IoT refers to a network of physical objects, devices, and sensors that communicate and exchange data over the internet. These objects can range from everyday appliances, such as smart refrigerators and thermostats to industrial machinery and environmental sensors. The IoT enables seamless data sharing, automation, and intelligent decision-making across various domains and finds applications in several sectors including industry, healthcare, smart cities, agriculture, and transportation.

A significant aspect of the IoT is the emergence of ZEDs. Unlike traditional devices that rely on batteries or external power sources, ZEDs operate without the need for recharging or replacing batteries or being connected to the electricity grid. Instead, they harvest energy from their surroundings, which makes them sustainable and environmentally friendly. ZEDs are innovative devices that utilize advanced technologies like Radio Frequency (RF) energy harvesting, backscatter communications, low-power computing, and ultra-low-power receivers [4, 5]. These technologies enable ZEDs to operate without conventional power sources, such as rechargeable lithium-ion batteries, disposable alkaline batteries, or continuous power from electrical outlets. This capability makes them ideal for use in remote or challenging environments. ZEDs play an essential role in unlocking the full potential of future networks, including 6G networks. By enabling battery-less operation, ZEDs contribute to a more sustainable communication architecture, addressing the energy consumption challenges posed by the growing number of connected devices.

Backscatter communication is an emerging research area, especially in low-power communication, with the potential for enabling a wide variety of IoT applications. A general system architecture is shown in Fig. 1.1a. It involves a transmitter, e.g., a base station, a Backscatter Device (BD), e.g., a ZED, and a receiver that, in some cases, can be co-located with the transmitter [6]. The transmitter emits an excitation or illumination signal, which is then reflected by the BD, and simultaneously modulated by changing its amplitude, frequency, and/or phase. Lastly, the receiver captures the backscattered signal and extracts the modulated information data.

A general BD architecture is given in Fig. 1.1b [7]. As shown, the BD is comprised of an antenna used to receive the excitation signal and transmit the backscatter signal, an energy harvester and Power Management Unit (PMU) used to harvest energy and power the device, a detector to detect the excitation signal, a microcontroller to control the load modulator and generate

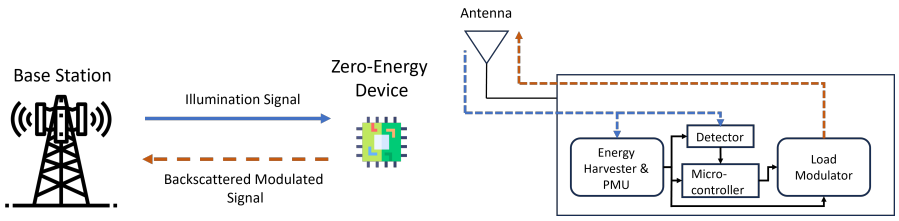

(a) (b)

Figure 1.1: (a) General backscatter communication system and (b) backscatter device architecture.

backscatter signals and finally the load modulator that changes the received signal characteristics and transmit data.

1.2 Problem

While backscatter communication offers significant advantages in terms of energy efficiency and low power consumption, it also faces several challenges. One critical issue is self-interference, where the carrier signal interferes with the receiver's ability to detect the backscattered signal. This creates interference, thereby compromising signal integrity and hindering accurate data decoding, indicating that self-interference is a significant bottleneck in the efficiency and reliability of such systems [8].

One way to address this problem is for the BD to utilize the harmonic frequencies of the illumination signal to modulate and transmit its data. By doing so, the problem of self-interference is eliminated, since the transmitted and received signals are in different frequencies.

Focusing on the integration of ZEDs into cellular IoT, one more aspect to investigate is addressing compatibility with current 5G and future 6G Orthogonal Frequency-Division Multiplexing (OFDM) base stations.

Taking into consideration the aforementioned problems, the research question this thesis seeks to answer is: How can harmonic backscattering be optimized to eliminate self-interference in zero-energy devices, enhancing communication with an OFDM-based base station or access node?

1.3 Purpose

The objective of the project is to implement a solution that addresses self-interference at the receiver by modeling the communication between an

OFDM-based transmitter and a ZED. The solution will be based on the harmonic generation at the ZED. Reduction of self-interference in backscatter communication systems is expected to be achieved through the strategic selection and optimization of an illumination signal, coupled with the implementation of a novel backscatter communication scheme based on harmonic backscattering. This approach is anticipated to reduce the Bit Error Ratio (BER) at the reader, as well as increase the Signal-to-Noise Ratio (SNR) performance to obtain a larger communication range, thereby improving the reliability and efficiency of the system.

The research conducted in this thesis is aligned with the interest of global companies in Ambient Internet of Things (AIoT) and adopting it in cellular networks. Specifically, 3GPP is currently running a study item on AIoT which includes both passive and active devices targeting the potential integration of these devices in existing 5G and future 6G networks. The problem studied in this thesis is highly connected to the global interest in AIoT as it investigates the self-interference problem for backscatter communication. In addition, the thesis studies and presents a possible solution for this problem based on harmonic backscattering which enables a base station or a User Equipment (UE) to act as the Carrier Wave (CW) transmitter and a backscatter receiver simultaneously, and hence, provides a step forward towards seamless integration of backscatter devices in existing cellular networks.

1.4 Goals

The goal of the project is to mathematically model the communication between a ZED and an OFDM-based transmitter by utilizing harmonic backscattering, and consecutively build a simulator to evaluate the system performance. This has been divided into the following subgoals:

1. **Mathematical modeling of the system.**
   This task entails modeling harmonic generation at the rectifier based on the selected OFDM-compatible waveform. An extended literature review shall be performed to achieve this task. The main system aspects that should be modeled are the waveform transmitted from the reader, the received signal at the tag and its harmonics to be used for transmission back to the reader, and finally the received signal at the reader.

2. **Analysis of the harmonic generation as the proposed solution.**
   One major challenge posed at this stage is understanding and controlling

the effects of Intermodulation (IM) products due to controlled harmonic generation on the Uplink (UL) waveform.

3. **Building a simulation model to verify the proposed solution.**
   The challenges that are anticipated at this stage are those associated with software development tasks, as well as time management. Simulation results might also indicate that there is a need for adjustments in the system modeling.

4. **Performance comparison of the proposed solution to existing ones**
   In the last stage of the project, we aim to compare the developed solution to existing ones, and especially normal backscattering by investigating and testing different scenarios.

1.5 Research Methodology

In the project, a combination of the experimental and applied research method [9] will be used, since the project involves manipulating variables and observing how these changes affect the system's performance, as well as collecting and analyzing data through simulations and testing.

Experimental research methodology was the first to be considered, since it enables the investigation of causal relationships between different parameters, such as the modulation scheme and the signal-to-noise ratio. By conducting controlled experiments and adjusting external parameters, it is possible to identify the key factors that influence system performance.

Applied research methodology is employed to bridge the gap between theoretical concepts and practical applications. In the context of this project, the applied research methodology is utilized in the process of the development and implementation of the proposed solution. By focusing on real-world applications and considering practical constraints, such as hardware limitations and environmental factors, this methodology ensures the relevance and applicability of the research findings.

The conceptual research method was also considered for this project since it can be used for theory development on novel concepts. However, it was deemed not suitable in the end, since it lacks the empirical validation of the findings.

1.6 Delimitations

This thesis, whilst focused on backscatter communication, falls under the category of a wireless communication system project. That means that it is bounded by the limitations that possible theoretical simplifications introduce, in comparison to the actual practical considerations that are made during real-life deployments. For example, a simplified channel and noise modeling can lead to less accurate results regarding the BER system performance. Such assumptions will be applied during the conduction of the thesis, since the focus is the fundamental modeling of harmonic backscattering and not the extension to more complex expressions that require further investigation on specific factors, such as the aforementioned channel modeling.

Furthermore, a physical implementation of the studied system is out of the scope of the thesis work, and hence, the developed techniques will not be tested with an actual base station of a cellular network.

1.7 Ethical considerations and sustainable development

There are a few ethics and sustainability aspects to consider while conducting this project. Sustainability goals are indirectly addressed by contributing to the development of low-power communication solutions, potentially reducing the environmental impact of battery-dependent devices. On the other hand, careful considerations need to be taken since increased adoption of zero-energy devices might lead to environmental concerns if not disposed of properly. As IoT technologies continue to advance, the project also aims to foster reduced power consumption in comparison to conventional wireless technologies.

From an ethical point of view, there are limited ways that a malicious actor could misuse the investigated technologies. One vulnerability is the manipulation of harmonic signals to gain unauthorized access or perform signal spoofing. For instance, one could mimic authorized devices to gain access to secure networks. In addition, one could intercept and decode backscatter signals for unauthorized access to transmitted information, thereby stealing sensitive data transmitted by IoT devices. These are challenges that can be addressed with careful privacy and security measures that include strong encryption mechanisms and secure communication protocols. However, this project's scope is not to provide a solution to these issues but to

focus on developing backscattering communication schemes.

1.8 Structure of the thesis

Chapter 2 presents relevant background information about backscatter and wireless communication systems. Chapter 3 presents the methodology used to solve the thesis problem, as well as details on the system modeling. In Chapter 4 we show the obtained results and conduct the necessary analysis to reach a conclusion in Chapter 5.

Chapter 2

Background

This chapter provides basic background information about backscatter communication, wireless power transfer, and energy harvesting. Additionally, this chapter describes important building blocks of general wireless communication systems and also references relative existing contributions in backscatter communication with a focus on the utilization of harmonics.

2.1 Backscatter Communication

Backscatter communication is a type of wireless communication that, in contrast to traditional wireless communication, relies on reflected or backscattered signals for communication. In this section, we will discuss the history, evolution, and basic principle of backscatter communication along with its different types and applications.

2.1.1 History and Operation

Communication by means of reflection was introduced by Alexander Graham Bell [10, 11] in 1880, when he developed the photophone, aiming to transmit speech via a beam of light modulated by sound waves. This early experiment laid the groundwork for subsequent innovations in reflective communication technology. In 1945, Leon Theremin created a covert listening device hidden within the Great Seal of the United States, employing a monopole antenna and resonant cavity to intercept and demodulate RF signals reflected from sound-sensitive membranes. Then, in 1948 Harry Stockman [12] introduced the concept of communication via reflections generated by mechanical devices, paving the way for modern applications of backscatter communication. Today,

contemporary tags utilize similar modulated backscatter principles, driving advancements in commercial applications. These historical developments showcase the evolution of reflective communication techniques, a vital part of modern wireless technologies.

The principle of backscatter communication can be likened to that of the heliograph [6], shown in Fig. 2.1. In the past, heliographs have been employed to reflect sunlight for communication, particularly in situations where alternative energy sources are unavailable, such as during camping or in remote locations. By manipulating the orientation of the mirror, one can send messages to distant recipients using Morse code. Similarly, backscatter communication operates by reflecting and modulating RF signals. A conventional backscatter communication system employs a backscatter tag that reflects an incoming excitation signal from a nearby transmitter, while simultaneously modulating its amplitude, frequency, or phase to encode information. The modulated signal is then received by a receiver and processed to extract the embedded data.

The primary mechanism behind the reflection of the incoming RF signal is impedance mismatching. It allows the BD to modulate the output signal by controlling the reflection coefficient, which is a measure of how much of an incident electromagnetic wave is reflected by the interface between two media. On a BD, impedance mismatch is achieved by connecting the antenna impedance to a load impedance. By adjusting the latter, the reflection coefficient is regulated making it possible for the device to toggle the reflected output signal among a set of amplitudes and phases. In practical BDs, this function is performed by a common electronic component called an RF switch.

Regarding the structure, in monostatic backscatter systems, the transmitter

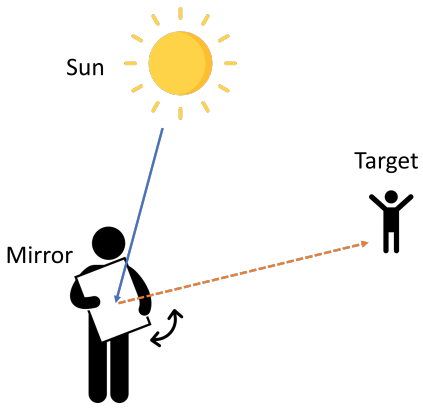

Figure 2.1: Illustration of the heliograph's operation.

and receiver are integrated, as seen in Radio Frequency Identification (RFID) readers. However, in bistatic backscatter designs, the transmitter and receiver are separated. Transmitters in bistatic systems can utilize ambient RF sources, such as TV or FM radio towers, cellular base stations, or Wi-Fi access points, providing flexibility in signal sources.

In the next subsection, the definitions of monostatic, bistatic, and ambient backscatter communication systems will be explored.

2.1.2 Categories of Backscatter Communication

Based on the architecture, backscatter communication systems can be divided into two main categories; monostatic and bistatic systems. A basic architecture for both is shown in Fig. 2.2. Depending on the excitation signal source, there can also be two different subcategories: dedicated source and ambient source systems. The final categorization is based on the type of the BD, which can be active, semi-passive, or passive [13]:

- **Active Devices**: These devices have their own internal power supply and a built-in transceiver. This allows them to actively generate and transmit signals, giving them a longer communication range compared to passive devices. Active devices are capable of both transmitting data actively and reflecting signals from other sources, which makes them versatile but also more complex and costly.

- **Semi-Passive Devices**: Semi-passive devices also come with an internal power supply, but unlike active devices, they typically only transmit data when they receive a signal from an external source. They combine elements of both active and passive systems, offering the advantage of longer communication ranges while still maintaining lower power consumption compared to fully active devices. They can use their internal power for operations like data processing and modulation but rely on external signals for transmission.

- **Passive Devices**: These devices do not have an internal power source (e.g., battery). Instead, they rely entirely on energy harvested from the environment, such as signals from an RFID reader or ambient RF sources, to power their operations. Due to this, passive devices have a simpler structure and are generally smaller and cheaper, but they have a limited communication range and are constrained by the availability of ambient energy sources. Passive devices are primarily used in

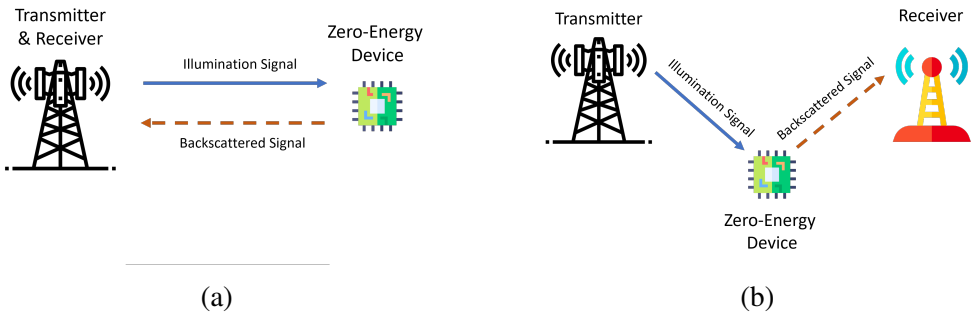

(a) (b)

Figure 2.2: Basic backscatter communication system architecture (a) Monostatic setup, (b) Bistatic setup.

applications where low power consumption and minimal maintenance are essential, such as in RFID tags.

In *monostatic systems*, only two elements are involved; a backscatter transmitter, that also acts as the receiver, and a ZED. An example of a popular monostatic backscatter system is the RFID system. The operation in such systems is as follows: the transmitter generates RF signals to illuminate the ZED, which in turn modulates the incoming signal and reflects it back to the receiver that is co-located with the transmitter. Monostatic systems are typically adopted for short-range applications due to their susceptibility to high round-trip path loss, combined with the challenge of distinguishing strong transmitted signals and weak backscatter signals [14].

In contrast to monostatic systems, the transmitter and the receiver in a *bistatic system* are separated, thereby eliminating the problem of round-trip path loss. One advantage over monostatic systems is that the communication range can be expanded since there exists the possibility of optimally placing the RF source. One of the drawbacks is that the deployment of dedicated transmitters is expensive. However, due to the simplification in component design, the manufacturing cost is reduced.

Ambient backscatter systems are similar in structure to bistatic systems, but instead of having a dedicated transmitter, they utilize any available ambient RF sources such as TV, cellular, or Wi-Fi signals. By doing so, the cost of deployment is diminished, and the need for a dedicated frequency spectrum is eliminated, thereby improving the spectrum resource allocation [7]. However, because of their unpredictability, ambient signals introduce a challenge in ensuring the performance stability of the system. Another challenge is that due to the lack of control in transmission power and placement of the RF source, the design of the system becomes more complicated.

2.1.3 Harmonic Backscattering

In recent years, harmonic backscattering has been investigated as a solution to either self-interference problems in monostatic setups or direct-link interference in bistatic setups. In contrast to regular backscattering communication systems, in harmonic backscattering, the backscattered signal is transmitted in a harmonic frequency range of the fundamental frequency used in the illumination signal [15]. One way to generate harmonic backscattering is to exploit the non-linearities present at the rectifier or the RF envelope detector integrated into the BD.

In Fig. 2.3, we illustrate how the concept of harmonic backscattering can be realized on a BD. One antenna receives the illumination signal, which is subsequently forwarded to a matching circuit, a Bandpass Filter (BPF), and the rectifier. Then part of the current is used to power the device and also perform the modulation of the backscatter signal that will carry the stored information. Another part of the current is used to exploit the generated harmonics at frequency $2f_o$ and be used as the backscatter signal that is in the end transmitted by another antenna.

2.1.4 Applications

Backscatter communications can be utilized in a variety of applications and also enable many future technologies, especially in the context of Zero-Energy (ZE)-IoT. As already mentioned one of the major applications is RFID systems that are widely deployed in numerous industries, such as in supply chain management to track products, identification cards to control access, or even in healthcare to track equipment location. Another application is wireless sensor networks where backscatter communication is employed for low-power communication between sensor nodes. These networks are used in

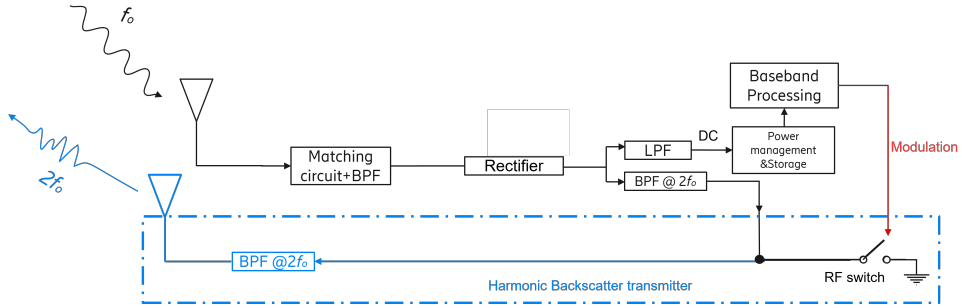

Figure 2.3: Concept of harmonic backscattering.

a variety of cases, such as smart agriculture, environmental monitoring, and industrial automation. A similar use-case area is wireless body area networks, in which wearable sensors are used for health monitoring. Last but not least, backscatter communication can be used in smart city infrastructure, enabling smart lighting, waste management, and other applications [15, 16, 17].

When looking into emerging technologies that will shape the future of connectivity, we can identify many that will be powered by backscatter communication. One is digital twins where sensors are needed to collect data from physical objects to create their digital versions. In addition, one can not avoid considering the possibilities that ZE-IoT will bring in conjunction with Artificial Intelligence (AI). Advanced sensors utilizing backscatter communication can employ low-energy AI for on-device preprocessing, thereby reducing the necessity for high-energy data transmission to central nodes. For instance, event cameras harness AI to efficiently process large volumes of data by transmitting only the most relevant information. In the future, ZE-IoT systems may incorporate approximate and intermittent AI computing, as well as energy-efficient technologies like neuromorphic AI, to strike a balance between computation and communication while minimizing energy consumption. Lastly, one fascinating future application is smart textiles that can be used in healthcare, sports, or even automotive safety to add functionality for the user [4].

2.2 Wireless Communication Systems

As backscatter communication foundations lie within the principles of wireless communications, in this section, we highlight the relevant background to foster a clear understanding of the system modeling that will be presented in Chapter 3. We begin with a general system architecture of a basic wireless system and continue with focusing on important building blocks, such as the modulation in Section 2.2.2 and wireless channel in Section 2.2.3. We end this subsection with a reference to OFDM, a substantial scheme used in modern digital communication systems.

2.2.1 General System Architecture

The block diagram of a basic wireless communication system is shown in Fig. 2.4. As depicted, it consists of some essential and some optional blocks.

The transmission stage begins with the *information source*, which could be either analog or digital. For instance, an analog signal source would be the

signal generated through a microphone capturing voice sound, and a digital source could be a computer generating binary data. The following optional step is to *encode* the information from the information source using encoding techniques, such as error correction coding or redundancy methods. This step ensures reliability since it enables error detection and correction at the receiver. Subsequently, the encoded information is modulated onto a carrier wave by passing through the *modulator*, which converts the digital signal to analog form suitable for transmission. Finally, the modulated signal is sent to the *transmission antenna* that converts electrical signals to electromagnetic waves for transmission through the *wireless channel* [18].

The modulated signal propagated through the wireless medium, which is affected by a variety of distortions, such as large-scale and small-scale path loss, as well as by interference factors. The channel also introduces attenuation to the signal strength and noise that corrupts the signal.

At the receiver side, there is a *receiving antenna* that captures the transmitted signal and forwards it to the *demodulator*, which extracts the modulated signal from the carrier wave. Next, the *decoder* attempts to reconstruct the original information data by reversing the encoding process performed at the transmitter, for example by employing error correction decoding algorithms such as the Viterbi or Reed-Solomon algorithm [19]. The recovered output of the decoder is finally used to estimate the transmitted information.

This is the fundamental flow for signal transmission and reception through a wireless channel. In practical and high-end systems, the complexity of the architecture increases to achieve reliability and adjust to the system requirements. For example, for a system to be complete, one should also consider security aspects, and thus, security measures include encryption and authentication to protect the wireless system from unauthorized access. Another important block would be a channel equalization block that could be used to mitigate the effects of multipath propagation and improve signal quality. If the system needs to support multiple users or signals, then multiple-access and multiplexing techniques are incorporated into the architecture to

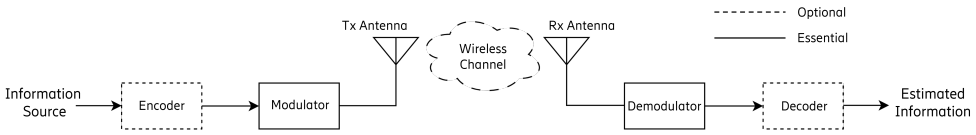

Figure 2.4: Block diagram of a standard wireless communication system.

enable concurrent transmission and reception.

In the next subsections, we dive deeper into the vital blocks that will be further examined in the thesis; the modulation stage and channel modeling.

2.2.2 Modulation

Modulation is a crucial stage in a wireless system as it provides a way of carrying information onto a carrier wave that can propagate through a wireless medium. Modulating baseband signals is necessary especially since they typically lie in a narrow low-frequency range. Modulation translates this frequency to a higher frequency range making it suitable for transmission through an antenna.

The choice of an appropriate modulation scheme depends on various factors such as bandwidth efficiency, required data rates, power efficiency, and robustness to noise and interference. In general, modulation can be achieved by controlling either the amplitude, frequency, or phase of the carrier signal and it can be either analog or digital. The difference in digital modulation is that the analog carrier is modulated by a digital signal. We refer to three relevant modulation schemes.

- **Amplitude Shift Keying (ASK)**

  ASK is one of the simplest digital modulation schemes. The main idea is to represent symbols by different amplitudes of the carrier frequency [20]. For example, in binary ASK, the two binary values are mapped to different amplitudes. One special case of ASK is On-Off Keying (OOK), usually employed by commercial RFID systems. In OOK the binary digit ”1” is encoded as the presence of the carrier signal, and ”0” is encoded as the absence of the carrier signal. Despite its susceptibility to noise and interference, ASK is a popular modulation scheme, since for the detection of the signal, only an envelope detection circuit is needed, thus making the signal detection simple [14, 21].

  The modulating signal $m(t)$ can be modeled as [22]

$$m(t) = \sum_{n=-\infty}^{\infty} m_n p(t - nT) \tag{2.1}$$

  where m_n are the binary symbols and $p(t)$ is defined as

$$p(t) = \begin{cases} 1, & 0 \leq t < \frac{T}{2} \\ 0, & \frac{T}{2} \leq t < T \end{cases}. \tag{2.2}$$

Since $p(t)$ is used as a periodic function in (2.1, it can be represented with its Fourier-series expression given in (2.3):

$$p(t) = \frac{1}{2} + \frac{2}{\pi} \sum_{n=1}^{\infty} \frac{1}{2n-1} \sin\left(\frac{(2n-1)\pi t}{T}\right). \tag{2.3}$$

- **Frequency Shift Keying (FSK)**

  In FSK, the symbols are represented by different frequencies. The simplest form of FSK is Binary Frequency Shift Keying (BFSK), in which the binary digit "1" is encoded as one frequency and "0" as another frequency. FSK is more tolerant to noise compared with amplitude modulation techniques [21], but requires more bandwidth. A special important form of FSK and more specifically of Continuous-Phase FSK (CPFSK) is Minimum Shift Keying (MSK), in which the spacing between the two frequencies is the minimum that can be used so that there are no phase discontinuities.

  BFSK can be modeled as [20]

$$s(t) = \begin{cases} A\cos(2\pi f_1 t), & \text{for binary "1"} \\ A\cos(2\pi f_2 t), & \text{for binary "0"} \end{cases} \tag{2.4}$$

  where f_1 and f_2 are the frequencies representing a binary "1" and "0" respectively.

  A square wave $x(t)$ can be considered as a more general expression for FSK that is given by

$$x(t) = \begin{cases} 1, & 0 \leq t < \frac{T}{2} \\ -1, & \frac{T}{2} \leq t < T \end{cases}. \tag{2.5}$$

  Taking into account two frequencies for FSK and their corresponding periods T_i, the Fourier series expression of $x(t)$ is written as

$$x_i(t) = \frac{4}{\pi} \sum_{n=1}^{\infty} \frac{1}{2n-1} \sin\left(\frac{(2n-1)\pi t}{T_i}\right). \tag{2.6}$$

For the special case of MSK the two frequencies are related by the following equations:

$$f_1 = f_c + \frac{1}{4T} \quad f_2 = f_c - \frac{1}{4T}. \tag{2.7}$$

- **Phase Shift Keying (PSK)**

  In PSK, the symbols are represented by different phase shifts of the carrier signal [20]. The simplest form uses two phases to encode two binary digits and it is referred to as Binary Phase Shift Keying (BPSK). Using PSK high data transmission rates can be achieved at the cost of more complicated signal recovery and receiver design [14].

  For BPSK, the same expression for a square wave as in (2.5) can be considered and the corresponding Fourier series expression in (2.6) but with only one period T.

In Fig. 2.5, the modulated signals of a simple sinusoidal carrier using the aforementioned modulation schemes are illustrated.

2.2.3 Channel Modeling

Wireless channels are subject to various phenomena that can cause fluctuations in the signal characteristics. These phenomena include reflection, diffraction,

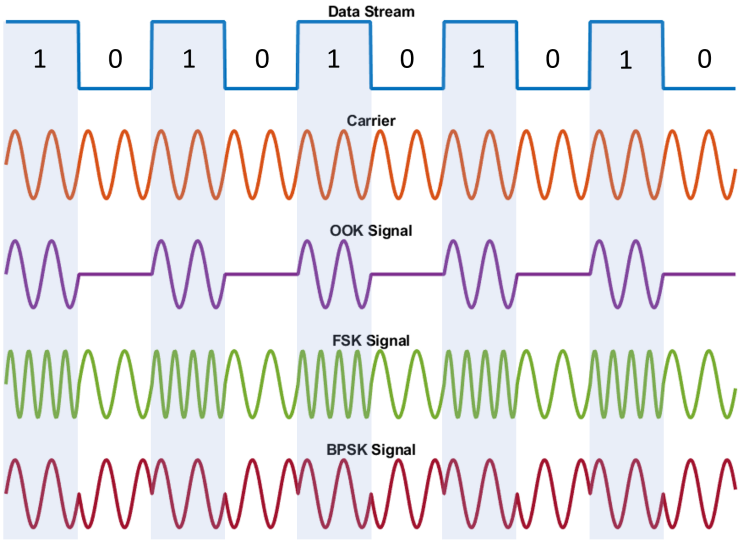

Figure 2.5: Illustrative example of OOK, BFSK, and BPSK.

scattering, and absorption of electromagnetic waves by objects in the environment. Other factors, such as atmospheric conditions, interference, and noise, can also affect the signal quality.

To estimate the properties of the channel, we use models that describe the aforementioned fluctuations. By modeling the channel, we can predict the channel's behavior and optimize the system's performance. The variations in the signal's characteristics are referred to as "fading". Fading can be categorized into two main types: large-scale fading and small-scale fading [23].

Large-scale fading refers to the long-term changes in signal strength due to the distance between the transmitter and the receiver or obstructions in a large environment. One key factor to consider in large-scale fading is path loss. As a signal travels over a distance, it spreads out and loses energy, resulting in attenuation in signal strength. The path loss is influenced by the distance between the transmitter and receiver and the frequency of the signal and can be modeled using the Friis free-space path loss model given by:

$$P_r = P_t G_t G_r \left(\frac{\lambda}{4\pi d}\right)^2 \tag{2.8}$$

where P_r is the received power, P_t is the transmitted power, G_t and G_r are the transmitter and receiver antenna gains respectively, λ is the wavelength, and d is the distance between the transmitter and the receiver.

The second key factor is shadow fading, which refers to the signal being "shadowed" by obstacles such as buildings, trees, and hills. These obstructions cause the received signal strength to vary slowly over relatively large distances. While the Friis model in (2.8) is valid for line-of-sight (free-space) channels where no shadowing occurs, in more realistic environments, shadowing becomes important. When modeling path loss for such cases, the general form of the Friis equation is used, but with a modified path loss exponent, which accounts for shadowing. Shadow fading is often modeled as a random process, with the received signal strength varying according to a log-normal distribution.

Small-scale fading refers to rapid fluctuations in signal strength over short distances or time durations. This type of fading is caused by the constructive and destructive interference of multiple signal paths, which is called multipath propagation. Note that the Friis equation does not account for multipath effects. This type of fading can be modeled by statistical models that characterize the variations in the signal's amplitude, phase, and delay.

We refer to some common wireless channel models.

- **Additive White Gaussian Noise (AWGN)**

  AWGN is a model of a noisy channel, where random noise is added to the signal being transmitted. The noise is modeled as a Gaussian distribution with zero mean. The term ”white” refers to the fact that the noise has a flat power spectral density across all frequencies. This means that it affects all frequencies equally, which can make it more challenging to distinguish the signal from the noise. The AWGN channel is commonly used in digital communications because it provides a simple and realistic model of the noise that is present in many real-world communication systems. The received signal with AWGN can be modeled as:

$$y = x + n \tag{2.9}$$

  where x is the transmitted signal, and n is the noise, modeled as a Gaussian random variable with zero mean and variance σ^2.

- **Rayleigh Fading**

  The Rayleigh fading model describes the case when there is no dominant signal path (like a direct line-of-sight between the transmitter and receiver), and instead, the received signal is the sum of multiple reflected, scattered, and diffracted signals. When numerous signals, each with random phases, add up, they produce a statistical phenomenon that follows a Rayleigh distribution with a Probability Density Function (PDF) given by:

$$p(r) = \begin{cases} \frac{r}{\sigma^2} e^{-\frac{r^2}{2\sigma^2}}, & 0 \leq r \leq \infty \\ 0, & r < 0 \end{cases} \tag{2.10}$$

  where σ is the RMS value of the received voltage signal before detection and σ^2 is the time-averaged power of the received signal before detection [19].

  Rayleigh fading is suitable for scenarios where multipath propagation dominates, such as urban environments with numerous obstacles, like buildings and trees.

- **Rice fading**

  Rice fading can be used to model the effect of multipath propagation. It is similar to the Rayleigh channel, but it assumes that there is a

dominant line-of-sight path in addition to the scattered paths, which are modeled as Rayleigh fading. The Rice fading model is characterized by a parameter called the K-factor, which determines the ratio of the power in the line-of-sight path to the power in the scattered paths. When the K-factor is large, the channel behaves more like a deterministic channel, with relatively little fading. When the K-factor is small, the channel behaves more like a Rayleigh channel, with significant fading. The Rician distribution is given by:

$$p(r) = \begin{cases} \frac{r}{\sigma^2} e^{-\frac{r^2+A^2}{2\sigma^2}} I_0\left(\frac{Ar}{\sigma^2}\right), & (A \geq 0, r \geq 0) \\ 0, & r < 0 \end{cases} \tag{2.11}$$

where A denotes the peak amplitude of the dominant signal and I_0 is the modified Bessel function of the first kind and zero-order [19]. The aforementioned K-factor is given by $K = \frac{A^2}{2\sigma^2}$ and is most commonly used in dB scale.

Rice fading is suitable for scenarios where both line-of-sight and multipath components coexist, such as suburban or rural environments.

Usually, the wireless communication channel is modeled using the channel coefficient h. This coefficient accounts for the effects of the channel on the transmitted signal, varying based on the channel conditions. For Rayleigh and Rice fading the received signal with noise can be modeled as:

$$y = hx + n \tag{2.12}$$

where $|h|$ follows either the Rayleigh or Rice distribution. Chapter 3 provides the expressions of the channel coefficients h for each investigated case.

2.2.4 OFDM

OFDM is a digital modulation technique used in modern communication systems. It is a multicarrier modulation scheme that divides the available frequency spectrum into many subcarriers, each carrying a separate data stream. These subcarriers are orthogonal to each other, meaning they are perfectly aligned in time and frequency, which reduces interference between them [23].

It is particularly useful in high-speed data transmission over wireless channels where the data rate is limited by multipath fading and interference.

By dividing the data into smaller subcarriers, OFDM can mitigate the effects of fading and interference, resulting in better spectral efficiency and higher data rates.

OFDM plays a crucial role in modern communication systems as it allows for efficient and reliable transmission of high-speed data over wireless channels. It is widely adopted in various wireless communication standards such as Wi-Fi, 4G LTE, and 5G. With the increasing demand for high-speed data transmission, OFDM is expected to continue playing a vital role in the development of future communication systems. Its ability to mitigate the effects of interference and fading makes it an ideal choice for wireless communication systems operating in challenging environments.

The key principle of OFDM is the orthogonality of subcarriers. Orthogonality ensures that even though the subcarriers overlap in the frequency domain, there is no inter-carrier interference. This is achieved by carefully selecting the subcarrier frequencies so that the integral of the product of any two different subcarriers over one OFDM symbol period is zero.

Mathematically, the transmitted OFDM signal can be represented in baseband as:

$$s(t) = \sum_{k=0}^{N-1} X_k e^{j2\pi k \Delta f t}, \quad 0 \leq t < T$$

where:

- X_k is the data symbol modulated onto the k-th subcarrier,
- N is the number of subcarriers,
- Δf is the subcarrier spacing,
- T is the duration of the OFDM symbol.

The subcarrier spacing Δf is chosen such that $\Delta f = \frac{1}{T}$, ensuring orthogonality.

The modulation process involves taking an Inverse Fast Fourier Transform (IFFT) of the data symbols, converting them from the frequency domain to the time domain. The demodulation process uses a Fast Fourier Transform (FFT) to convert the received signal back to the frequency domain.

A block diagram of an OFDM system is illustrated in Fig. 2.6. The operation is described as follows:

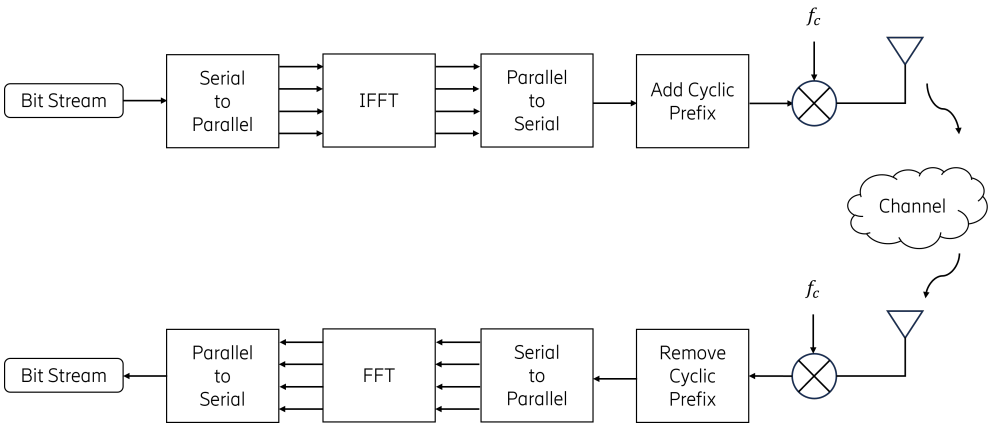

Figure 2.6: Block diagram of an OFDM transceiver.

1. The process begins with a serial-to-parallel conversion of the data stream, where individual samples from each carrier are grouped into an OFDM symbol. Each value in this group represents the weight for its corresponding subcarrier.

2. Following this, the IFFT transforms these values into a time-domain data stream for transmission, effectively combining the subcarriers in the process. It's the IFFT's role to prevent interference between the subcarriers. Additionally, a cyclic prefix is added to the signal to mitigate inter-symbol interference (ISI) caused by multipath propagation.

3. Later, the time-domain data stream is converted back into a serial stream through a parallel-to-serial operation and then modulated onto a carrier of frequency f_c using a single oscillator.

4. Upon reaching the receiver end, the process is reversed. The cyclic prefix is removed to restore the original signal and then an FFT module maps the incoming signal back to the subcarriers, allowing the data streams to be recovered by retrieving the weights for each subcarrier from each sample.

2.3 Related Work

Backscattering communication is a rather popular field of research supported by a vast amount of publications that were ignited during the Second World

War [13] and are still in bloom today. In this section, we present some of the most recent and relevant to the thesis works that have been published. Since the focus of the thesis is self-interference mitigation and integration with OFDM, we will mainly discuss studies that are targeting these challenges, as well as studies that perform a theoretical analysis of the system models. We begin by discussing publications on regular backscatter communications for both monostatic and bistatic systems, we continue by highlighting works on harmonic backscattering, and we end this section by referring to publications that focus on OFDM adoption for the illumination signal. Although, it does not constitute the focus of the thesis, works on ambient backscattering are also being considered. To the author's knowledge, there has not been work in the literature that combines harmonic backscattering with an OFDM-based illumination signal.

2.3.1 Regular Backscattering

Studies on regular backscattering are highly concentrated on the RFID technology and have been attracting attention from the research community for many years. We refer to some of the most recent studies.

In [24], Kimionis, Bletsas, and Sahalos present a bistatic architecture with the potential to be employed in Wireless Sensor Networks (WSNs). The authors propose receiver designs based on OOK and FSK that overcome the frequency offset between the transmitter and the receiver and simultaneously refer to non-coherent receivers. The work focuses on deriving theoretical expressions to model the signals for the bistatic backscatter systems and obtain an expression for the BER. Experimental results show that a communication range of up to 130 m can be achieved with 20 mW carrier power.

A novel backscatter communication system, called BackFi, for long-range communication between low-power backscatter IoT sensors and WiFi access points, is presented in [25]. The key contributions of the study include a low-power IoT sensor design capable of sustaining high data rates and a novel WiFi access point radio circuit design that can receive backscatter signals while transmitting WiFi packets. The system exploited ambient WiFi signals and utilized self-interference cancellation techniques and advanced decoding algorithms to enhance signal reception and processing, which led to improved throughput and communication range. Results demonstrated that BackFi achieved a high throughput of 1-5 Mbps at ranges of 1-5 m, outperforming existing WiFi backscatter systems.

Another system utilizing ambient signals was proposed in [26]. The

authors introduce Bluetooth Low Energy (BLE)-Backscatter technology as an innovative approach for ultralow-power data uplink from sensor nodes to existing BLE-enabled smartphones and tablets without the requirement for any modifications to their hardware or software. In the paper, Ensworth and Reynolds present the development of a standalone BLE-Backscatter tag that demonstrates successful reception of backscattered BLE advertising packets by unmodified BLE devices. Experimental results showcase a significant reduction in energy consumption per bit transmitted compared to conventional BLE transmitters, highlighting the energy efficiency of the BLE-Backscatter concept.

Important research has also been conducted regarding the derivation of theoretical expressions for signal modeling in backscatter systems. In [27], the authors study the waveform design for Wireless Power Transfer (WPT) and highlight the modeling of the non-linearity present at the rectifier. In [28], Mouris et. al investigated multi-tone signals for WPT and studied non-linear energy harvesting models. Solutions based on a second-order polynomial curve-fitting model and a linearly constrained quadratic program problem formulation are presented, highlighting the importance of optimizing the design of multi-tone signals.

2.3.2 Harmonic Backscattering

There are several available studies on harmonic backscattering. Currently, most of them are hardware-oriented solutions, while others focus on the general architecture of the backscatter system.

In [29], Ma, Hui, and Kan present the first harmonic RFID system integrated with a Wireless Identification and Sensing Platform (WISP). The proposed platform is designed to suppress self-jamming and reduce reader-to-reader interference. The paper focuses on introducing a novel circuit architecture, referred to as Harmonic-WISP, suitable for seamless integration with WISP without affecting the tag sensitivity or the harmonic generation efficiency. The second harmonic of the fundamental frequency is used for the uplink signal, and ASK modulation is applied at the backscatter tag. The study results show that Harmonic RFID systems offer a significant improvement of 13.56 dB in Signal-to-Interference Ratio (SIR) compared to conventional RFID. The authors verify the operation of the proposed architecture with measurements that test the reading range and tag communication.

A class-3 Ultra High Frequency (UHF) RFID system based on harmonic backscattering for long read-range applications is developed by Chen et al. in

[30]. Harmonic backscattering was chosen in the paper as a solution to address carrier leakage issues in UHF RFID readers. The system implementation was based on a software-defined radio platform for the reader and a novel semi-passive RFID tag with -20 dBm sensitivity for the backscatter device. Results show that a system sensitivity of -101 dBm is achieved for a 20 m communication distance and ideal channel conditions, showcasing the benefits of the use of harmonic backscattering in such systems.

A different solution to conventional UHF RFID challenges, such as self-jamming and multi-path interference is proposed in [31], where Kumar et al. present the design of an additional RF interface layer between the reader and the tag. The role of this interface layer is to transmit the illumination signal at the fundamental frequency, receive the backscatter signal in the 3rd harmonic frequency, and downconvert it to be sent to the reader. At the same time, they propose a new design for a dual-band antenna that can be integrated with a conventional RFID tag to increase the radiation efficiency of the tag. The advantage of the proposed solution is that it can be deployed without any internal adjustments in the design of a conventional UHF RFID reader. Experiments showed that a reduction of 30 dB in noise levels can be reached by utilizing the harmonic frequency. Overall the suggested platform achieves higher SNR and wider bandwidth in comparison to the conventional system, showcasing the benefits of self-jamming cancellation. However, the authors note that adjustments in the RFID protocol should be considered to fully exploit the potential for wider bandwidth

A novel Simultaneous Wireless Information and Power Transfer (SWIPT) architecture based on incorporation of third-order intermodulation backscattering is presented in [32]. More specifically, the authors propose a solution for eliminating self-interference at the reader by using a Frequency Division Duplex (FDD)-multitone SWIPT architecture. The operation they describe is as follows: A multi-tone signal carrying the downlink data is received by the proposed circuit, which in turn backscatters the third-order IM product for the uplink signal. In that way, the downlink and uplink data lie in different frequency bands. In the paper, the authors perform a multi-tone analysis and derive expressions that relate the Peak-to-average Power Ratio (PAPR) to the input signal. In addition, they design the circuit for FDD SWIPT and perform experiments that verify the operation. The proposed architecture enhances SWIPT performance, achieving a 10.1 dB IM3 backscattering dynamic range and 25.5% power conversion efficiency when the RF power consumption is at 7.94 μW. The joint operation demonstrates a peak power conversion efficiency of 42.8% at -6 dBm power, with an 8.5% increase in energy harvesting

efficiency using a frequency-modulated signal.

To the author's best knowledge, the present literature on harmonic backscattering lacks a proper communication system model that accounts for the illumination signal type, wireless channel, non-linear harmonic generation, modulation, and detection methods. Having such a model facilitates studying and designing harmonic backscatter systems as well as evaluating their performance. The main contribution of this thesis lies in providing a comprehensive mathematical model for harmonic backscattering and evaluating its performance against regular backscattering.

2.3.3 Compatibility with OFDM

Recently, there have been a few studies on integrating OFDM in backscatter communication systems. In [33], the authors present a system model for ambient backscatter communications over ambient OFDM carriers and showcase an optimal transceiver design. The challenges in the study were mitigating the impact of direct-link interference, ensuring effective synchronization, and estimating the backscatter channel. In the paper, the authors also provide a closed-form expression for the optimal threshold detection and the BER for a maximum-likelihood detector. In addition, the proposed ambient backscatter system features efficient timing synchronization algorithms. The system's transmission rate and detection performance are analyzed and simulation results demonstrate that the proposed design outperforms conventional designs based on energy detection, with higher transmission rates, better BER performance, and an extended operating range.

In [34], Lopez, He, and Khan propose a novel non-ambient OFDM-based carrier waveform design for a bistatic backscatter system. The authors present a method to achieve orthogonality between OFDM signals originating from the transmitter and the BD, while also proposing a novel scheme to generate a backscattered signal with BPSK or a higher-order PSK modulation. Simulation results show that the proposed solution is suitable for integration of backscatter communication in cellular IoT.

2.4 Summary

This chapter has described backscatter communication systems and important relevant elements in a general wireless communication system. It has also presented recent advancements in the research field and has built the foundation for understanding the system modeling followed later in the thesis.

Among others, in this chapter, the importance of theoretical modeling and experimental validation of the system was highlighted.

We can summarize the categories of the mentioned systems as follows; We first differentiate between regular and harmonic backscattering and then identify monostatic or bistatic setups for each case. For a bistatic setup, either a dedicated or an ambient RF source can be considered as the illumination signal regardless of the backscatter type.

In the next chapter, we analyze the system modeling that was utilized in the project and distinguish investigation cases.

Chapter 3

System and Signal Modeling

3.1 System Model

In this project, we consider two backscatter communication models shown in Fig. 3.1.

(a) *Monostatic Backscatter System*

The first one is a monostatic backscatter system consisting of a Carrier Emitter (CE) node that is co-located with the Reader (RD) node, and a BD.

(b) *Bistatic Backscatter System*

The second one is a bistatic backscatter system consisting of a CE, a separate RD, and a BD.

In both systems, the CE has a dedicated, controllable RF source and transmits a CW or *illumination signal* that is being received by the BD. The received signal at the BD has two purposes; first, to be used for energy harvesting to power the BD and second to be modulated by the BD and then used to transmit its data. The backscattered signal is then being received by the RD. The difference between the two systems is that in the case of the monostatic system, the RD and CE are placed on the same device, while in the bistatic system, they are separated.

The CE and RD are assumed to be OFDM compatible meaning they can transmit or receive OFDM signals. In their general form, OFDM signals can be modeled as multi-tone signals [23].

Since the signal modeling for the two systems is the same, we are performing the analysis only once. We consider a CE with M antennas and

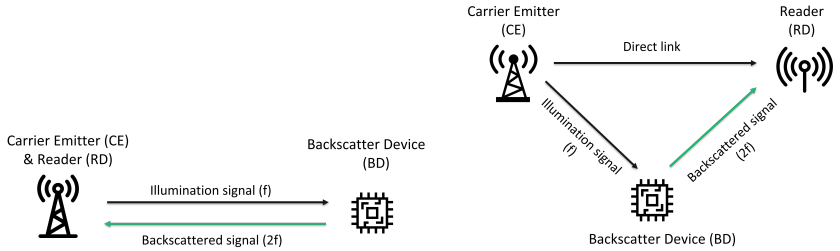

(a) Monostatic (b) Bistatic

Figure 3.1: Backscatter systems under consideration.

N sinewaves. Similar to [27], we can model the multi-tone CW at time t on antenna m as

$$x_m(t) = \Re\left\{\sum_{n=0}^{N-1} w_{n,m} e^{j2\pi f_n t}\right\} \tag{3.1}$$

with $w_{n,m} = s_{n,m}e^{j\phi_{n,m}}$ where $s_{n,m}$ and $\phi_{n,m}$ represent the amplitude and phase of the nth sinewave at frequency f_n on antenna m, respectively.

All transmit signals can be written as a transmit signal vector, denoted by $\mathbf{x}(t)$ and expressed as

$$\mathbf{x}(t) = \Re\left\{\sum_{n=0}^{N-1} \mathbf{w}_n e^{j2\pi f_n t}\right\} \tag{3.2}$$

where $\mathbf{w}_n = [w_{n,1} \dots w_{n,M}]^T$.

We also assume a multipath channel with a frequency response modeled by the channel vector $\mathbf{h}_n = [h_{n,1} \dots h_{n,M}]^T$ and then assuming that the BD is equipped with a single antenna and neglecting the noise, we express the received signal at the BD as

$$y(t) = \Re\left\{\sum_{n=0}^{N-1} \mathbf{h}_n^T \mathbf{w}_n e^{j2\pi f_n t}\right\} \tag{3.3}$$

.

3.2 Rectifier Modeling

The next step is to model the signal after it is received by the BD. For that reason, we need to model the rectifier incorporated into the BD. We assume the antenna is lossless and modeled as an equivalent voltage source $V_s(t)$ in

series with an impedance R_A. The antenna equivalent circuit and the single diode rectifier assumed in this analysis are shown in Fig. 3.2.

Under perfect matching, the received power P_s is completely transferred to the rectenna's input impedance R_{in} and so

$$P_s = \frac{\mathbb{E}\left\{|V_{in}(t)|^2\right\}}{R_{in}} = \mathbb{E}\left\{y^2(t)\right\}. \tag{3.4}$$

Here the expectation is used to estimate the average power. Since we have a voltage divider, we have the following:

$$V_{in} = \frac{R_{in}}{R_{in} + R_A} \cdot V_s \overset{R_{in}=R_A}{\Rightarrow} V_{in} = \frac{V_S}{2} \tag{3.5}$$

$$V_{in}(t) = \sqrt{R_{in}} \cdot y(t) \Rightarrow V_{in}(t) = \sqrt{R_A} \cdot y(t) \tag{3.6}$$

$$V_s(t) = 2V_{in}(t) \Rightarrow V_s(t) = 2\sqrt{R_A} \cdot y(t) \tag{3.7}$$

If we consider the rectifier model, we have the following for the voltage $V_d(t)$ at the diode and the generated current $i_d(t)$:

$$V_d(t) = V_{in}(t) - V_{out}(t) \tag{3.8}$$

$$i_d(t) = i_s\left(e^{\frac{v_d(t)}{nu_t}} - 1\right) \tag{3.9}$$

where i_s is the reverse bias saturation current, u_t is the thermal voltage and n is the ideality factor of the diode.

In order to capture the non-linearity of the diode, we apply the Taylor expansion to (3.9). Therefore, we can express the current $i_d(t)$ flowing through the diode through [27]:

(a) Antenna equivalent circuit

(b) Single diode rectifier

Figure 3.2: Receiving antenna and rectenna at the BD.

$$i_d(t) = \sum_{i=0}^{\infty} k_i \left(u_d(t) - a\right)^i \tag{3.10}$$

with $k_0 = i_s \left(e^{\frac{a}{u_t}} - 1\right)$ and $k_i = i_s \frac{e^{\frac{a}{u_t}}}{i!(n \cdot v_t)^i}, i = 1, \ldots, \infty$.

For simplicity, we can assume that the diode delivers a constant output DC voltage a, where $a = \mathbb{E}\left\{V_{in}(t) - V_{out}(t)\right\} = -V_{out}$, and so the resulting Taylor expansion becomes

$$i_d(t) = \sum_{i=0}^{\infty} k_i V_{in}(t)^i = \sum_{i=0}^{\infty} k_i R_A^{i/2} y(t)^i \tag{3.11}$$

.

Now in (3.11) we have an expression that relates the diode current $i_d(t)$ to the incident signal $y(t)$ on the BD. The Taylor expansion is terminated at the second non-linear term to analyze the harmonics and the IM products.

From (3.11) we get

$$i_d(t) = k_0 + k_1 \sqrt{R_A} y(t) + k_2 R_A y^2(t) \tag{3.12}$$

.

3.2.1 Harmonic Analysis and Intermodulation Products

Following the derivation of the general expression outlined in (3.12), it is possible to proceed with a harmonic analysis to explore the utilization of the harmonic signal and identify potential frequency overlaps. In Section 3.2.1.1, we begin with the general expression of the multi-tone signal that can also be used to represent an OFDM signal. Subsequently, in Section 3.2.1.2 we provide a special-case analysis for a two-tone signal for the sake of simplicity.

3.2.1.1 General Multi-tone Signal

From (3.3), we can write

$$y(t) = \sum_{n=0}^{N-1} A_n \cos(2\pi f_n t + \delta_n) \tag{3.13}$$

where N is the number of sinewaves or tones, A_n and δ_n are the amplitude and the phase of the n_{th} tone, respectively.

At this point, considering that

$$\cos^2 x = \frac{1}{2} + \frac{1}{2}\cos(2x), \tag{3.14}$$

and that

$$\cos a \cos b = \frac{1}{2}[\cos(a+b) + \cos(a-b)], \tag{3.15}$$

we obtain an expression for $y^2(t)$ given in (3.16):

$$y^2(t) = \frac{1}{2}\sum_{n_0,n_1} A_{n_0}A_{n_1}[\cos(2\pi f^{++}t + \delta^{++}) + \cos(2\pi f^{+-}t + \delta^{+-})] \tag{3.16}$$

where

- $n_0, n_1 \in \mathbb{Z}, \quad 0 \leq n_0, n_1 \leq N-1$
- $f^{++} = f_{n_0} + f_{n_1}$ and $\delta^{++} = \delta_{n_0} + \delta_{n_1}$
- $f^{+-} = f_{n_0} - f_{n_1}$ and $\delta^{+-} = \delta_{n_0} - \delta_{n_1}$.

3.2.1.2 Two-Tone Signal

Let's assume that $y(t)$ is a two-tone signal. Then, from (3.16) for $N = 2$, we obtain a mathematical expression for $y(t)$ in (3.17):

$$y(t) = A_0\cos(2\pi f_0 t + \delta_0) + A_1\cos(2\pi f_1 t + \delta_1) \tag{3.17}$$

First, we calculate the expression for $y^2(t)$:

$$\begin{aligned} y^2(t) &= [A_0\cos(2\pi f_0 t + \delta_0) + A_1\cos(2\pi f_1 t + \delta_1)]^2 \\ &= A_0^2\cos^2(2\pi f_0 t + \delta_0) + 2A_0A_1\cos(2\pi f_0 t + \delta_0)\cos(2\pi f_1 t + \delta_1) \\ &+ A_1^2\cos^2(2\pi f_1 t + \delta_1) \end{aligned}$$

Using (3.14) and (3.15) we get

$$\begin{aligned} y^2(t) = \frac{1}{2}(A_0^2 + A_1^2) &+ \frac{1}{2}A_0^2\cos(2\pi 2 f_0 t + 2\delta_0) + \frac{1}{2}A_1^2\cos(2\pi 2 f_1 + 2\delta_1) \\ &+ A_0A_1\cos[(2\pi f_0 + 2\pi f_1)t + \delta_0 + \delta_1] \\ &+ A_0A_1\cos[(2\pi f_0 - 2\pi f_1)t + \delta_0 - \delta_1] \end{aligned} \tag{3.18}$$

From (3.18) it is evident that the 2nd order IM products will affect the uplink signal. In the next subsection, we investigate the potential problems by performing a frequency analysis.

3.2.1.3 Frequency Mapping

As mentioned in Chapter 2, the BD has a switch that toggles between two load impedances and connects the antenna impedance to either one. As a result, the signal frequencies are shifted by the amount of the switching rate [35]. For that reason, it is of great significance to analyze how the switch will affect the harmonic frequencies and to which frequencies the IM products will be mapped. we define a few important variables for our analysis:

- Δf: **Subcarrier Spacing**
  The OFDM predefined subcarrier spacing. It depends on the available bandwidth and number of subcarriers N.
- f_s: **Switching Rate**
  Adjustable switching rate of the backscatter radio. It will affect the impinging signal frequencies $(f \pm f_s)$. For OFDM compatibility, we assume $f_s = m\Delta f\ , m \in \mathbb{Q}$ [34].
- $f_i, i = 1, \ldots, N$: **Subcarrier Frequencies**
  Frequencies of all subcarriers. Note that in OFDM: $f_{i+1} = f_i + \Delta f$.

In Fig. 3.3, we can see the frequencies of the fundamental signal $y(t)$ and the harmonic signal $y^2(t)$, and in the zoomed-in area, we illustrate the mixed frequencies after the switch at the backscatter radio. The yellow dashed-dotted line represents the DC component, the black solid line the fundamental frequencies and the green dashed line the harmonic frequencies and IM products. The corresponding amplitude is shown at the top of the arrowed lines.

In the zoomed-in area, the mixed harmonic frequencies are shown in dashed-dotted purple and dotted red. From Fig. 3.3, we can already observe a potential frequency overlap between the mixed harmonic frequencies (purple dash-dotted lines) and the mixed IM products (red dotted lines). This overlap depends on the choice of the switching rate f_s, as well as the frequency spacing between f_{n_0} and f_{n_1}.

Based on this analysis, it is evident that the overlap will not occur if:

$$f_{n_0} + f_{n_1} + f_s < 2f_{n_1} - f_s \Rightarrow f_s < \frac{\Delta f}{2} \tag{3.19}$$

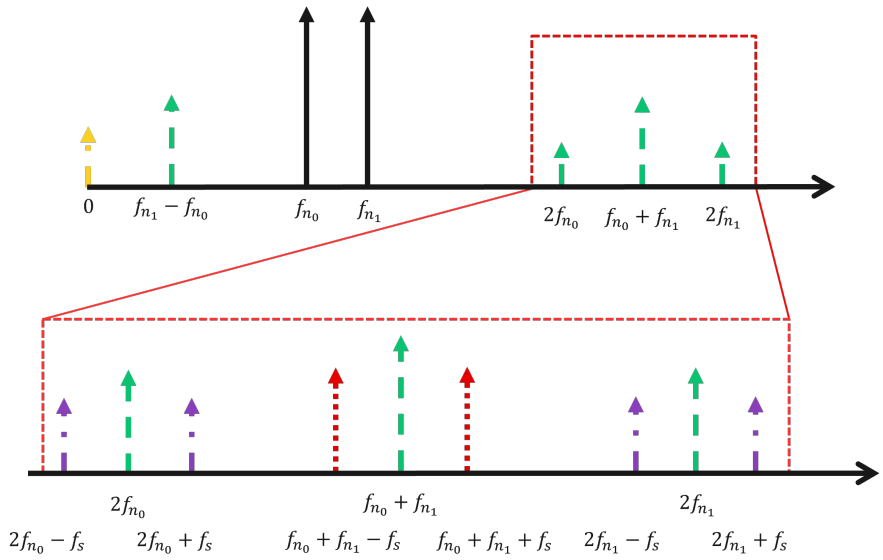

Figure 3.3: Illustration of frequencies in the fundamental and harmonic signal.

3.3 Backscatter Modulation

At this stage, we have the harmonic signal that will carry the BD data. The next step is for the BD to modulate the data. A modulation signal $m(t)$ will modulate the harmonic carrier signal $c(t) = y^2(t)$, resulting in the final reflected backscatter signal $z(t)$ that will be transmitted from the BD. In this project, we choose to investigate the utilization of ASK, one of the modulation schemes presented in Chapter 2. The reason behind this decision is the simplicity of this modulation scheme both in the procedure and the implementation on the BD, which significantly reduces the cost and complexity of the device.

The simplest form of ASK is OOK, as mentioned in Section 2.2.2. We opt to utilize OOK with unipolar Manchester encoding due to its numerous advantages in improving signal reliability compared to standard OOK and simplifying the demodulation process. Manchester encoding is a type of digital encoding technique that merges data and clock signals into a single self-synchronizing data stream. It is characterized by having a transition in the middle of each bit period, which helps maintain synchronization between the transmitter and the receiver. Manchester encoding inherently provides self-clocking, allowing for synchronization without the need for a separate clock signal. It also ensures a balanced DC component, which prevents

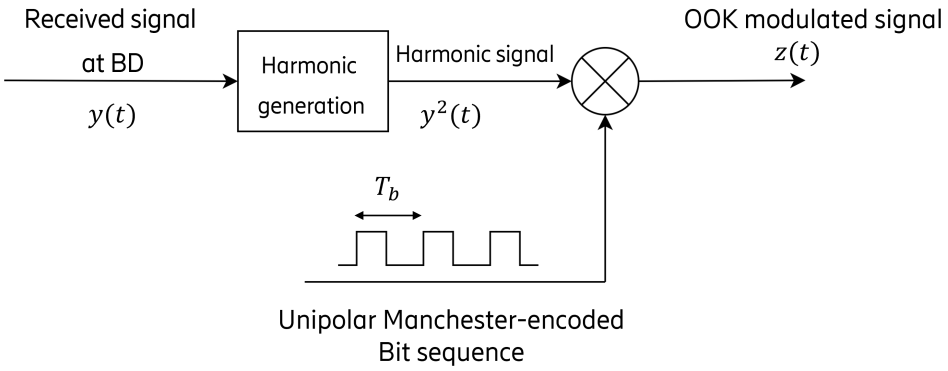

Figure 3.4: Block diagram of the OOK-based modulator used in the system.

extended periods of high or low signals, enhancing transmission stability. Furthermore, the regular transitions within the encoded signal help with error detection, making the system more resilient against noise and timing errors. These transitions also simplify demodulation, as they are easier to detect and decode. There are two main conventions for Manchester encoding; the first one was introduced by G.E. Thomas and represents a logical '1' with a high-to-low transition and a logical '0' with a low-to-high transition [36]. The second one is the IEEE 802.3 (Ethernet) convention, in which a logical '0' is represented by a high-to-low transition in the middle of the bit period, while a logical '1' is represented by a low-to-high transition [37]. In our system, to implement Manchester encoding, we follow the definition given by G.E. Thomas. Specifically for unipolar Manchester coding, low is defined as zero level.

In Fig. 3.4, the architecture of the modulator used in the BD is illustrated. After the signal has been received by the BD, we get the second harmonic signal generated by the non-linearities of the rectifier and multiply it with the unipolar Manchester encoded bit sequence of period T_b stored in the BD, and we derive the final modulated signal that is to be transmitted from the BD. It should be noted that $T_b = \frac{2}{f_s}$, since for Manchester encoding there is a transition within the bit period.

3.4 Channel Modeling

The modulated signal is then transmitted by the BD to the RD, which extracts the information from the signal. This transmission occurs over a wireless channel, which requires accurate modeling to understand its behavior

and optimize communication performance. We test three different channel conditions, all of which are described in Chapter 2. We consider an AWGN channel, a Rayleigh fading channel, and a Rician fading channel. In all three cases, we incorporate the corresponding path losses in the final model.

In an AWGN channel, the channel coefficient is simply $h = 1$, as there is no fading, and the only impairment to the signal is the addition of random Gaussian noise.

In a Rayleigh fading channel, the coefficient h is a complex random variable representing the sum of many scattered multipath components. Both the real and imaginary parts of h are modeled as independent Gaussian random variables with zero mean and variance $\sigma^2/2$. The Rayleigh channel coefficient is given by

$$h_{\text{Rayleigh}} = h_{\text{re}} + jh_{\text{im}} \tag{3.20}$$

where $h_{\text{re}} \sim \mathcal{N}(0, \sigma^2/2)$, $h_{\text{im}} \sim \mathcal{N}(0, \sigma^2/2)$.

The magnitude of h_{Rayleigh} follows the Rayleigh distribution.

As mentioned in Chapter 2, a Rice fading channel includes a dominant LOS component along with the scattered components. The channel coefficient h is modeled as the sum of a complex-valued LOS component and a Rayleigh-distributed scattered component. The LOS component has a fixed amplitude and a random phase uniformly distributed between 0 and 2π. The scattered component is similar to the Rayleigh fading case, resulting in the following expression for the Rice channel coefficient:

$$h_{\text{Rice}} = Ae^{j\theta} + h_{\text{sc}} \tag{3.21}$$

where $h_{\text{sc}} = \sqrt{\frac{1}{K+1}}\left(h_{\text{re}} + jh_{\text{im}}\right)$, $A = \sqrt{\frac{K}{K+1}}$, $\theta \sim \mathcal{U}(0, 2\pi)$ Here, A represents the amplitude of the LOS component, which is scaled by the Rice factor K, and θ is the random phase of the LOS component. As $K \to 0$, the Rice fading model reduces to the Rayleigh fading model, while large K-values indicate a dominant LOS path.

3.5 Receiver Design

After the signal is transmitted by the BD, it reaches the receiver back at the RD. In our system, we design a baseband receiver that performs envelope detection for the received signal, which is a non-coherent method of demodulating OOK signals.

In Fig. 3.5, the block diagram of the demodulator is illustrated. The

process begins with the downconvertion of the received signal achieved by multiplying it with a cosine signal at the carrier frequency f_c. For harmonic backscattering, this frequency corresponds to the second harmonic frequency. Once the baseband signal is obtained, we perform envelope detection, which is a crucial step in demodulation.

Envelope detection is used to extract the original information signal from the modulated carrier. It involves obtaining the absolute value of the baseband signal. This step effectively strips away the high-frequency components, leaving behind the varying amplitude or "envelope" of the original signal. The envelope represents the variations in amplitude that were imposed on the carrier during modulation, thus carrying the information content of the signal.

To make bit decisions, we sample the signal at every bit period, capturing the signal form for each bit. At this point, we follow a decoding procedure based on the unipolar Manchester encoding used during modulation. We split the signal into two halves and calculate the energy of each half. If the energy in the first half is greater than in the second half, it indicates a transition from high to low, which corresponds to a bit value of 1. Conversely, if the energy in the second half is greater, it indicates a transition from low to high, corresponding to a bit value of 0. This decoding process is repeated iteratively until a decision is made for all bits.

3.6 Interference Modeling

This section describes the interference modeling that needs to be taken into account when comparing regular backscattering to harmonic backscattering. Unlike harmonic backscattering, regular backscattering involves having to differentiate between interference signals and the information signal, since

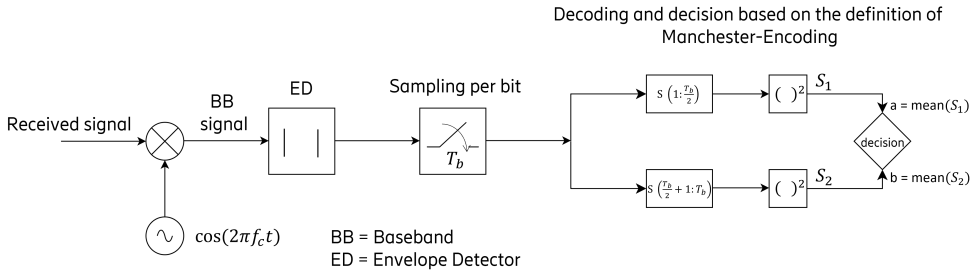

Figure 3.5: Block diagram of the envelope detection-based demodulator used in the system.

both are transmitted in the same frequency.

The type of interference differs between monostatic and bistatic setups. In the monostatic setup, the interfering signal is the carrier leakage at the receiver, while in the bistatic setup, it is the direct-link signal from the transmitter received at the RD. In this project, we attempt to regulate these interference signals in similar but distinct ways. For the monostatic setup refer to it as Carrier Leakage Suppression (CLS), and for the bistatic setup as Carrier-to-Interference Ratio (CIR).

3.6.1 CLS

In a monostatic setup, carrier leakage is present due to the inherent design of the system. Since a single antenna is used for both transmitting and receiving signals, the following issues may arise:

- Signal Reflection

  When the CE emits a signal, part of this signal can reflect back towards the antenna, creating a situation where the transmitted carrier frequency can mix with the received signal. This reflection can cause the carrier signal to be detected alongside the backscattered signal, leading to carrier leakage.

- Coupling

  In a monostatic setup, there is often a strong coupling between the transmitting and receiving paths. This means that the transmitted signal can directly reach the receiving circuitry, either through the antenna or through unintended paths, contributing to carrier leakage.

- Component Imperfections

  Imperfections in the electronic components, such as imperfect isolation between the transmitter and receiver, can also cause leakage of the carrier signal into the receiving path.

Carrier leakage can interfere with the detection of weak backscattered signals, making it challenging to accurately decode the information. To mitigate this issue, designers employ various techniques such as using filters, improving antenna design, and applying signal processing algorithms to distinguish between the carrier and the backscattered signals. In general, this is a highly complicated process and may require advanced interference

cancellation methods, for example implementing full-duplex operation to manage self-interference in monostatic setups. This complexity makes harmonic backscattering particularly appealing, as it avoids these interference issues by operating on a different frequency band, simplifying the receiver design and reducing costs. In our project, we model the effect of the mitigation techniques as a level of suppression in the dB scale. Essentially, CLS is modeled as a factor of attenuation for the interference signal.

3.6.2 CIR

In the bistatic setup, the direct signal from the transmitter can leak into the receiver channel, creating interference that overlaps with the backscattered signal from the BD. This direct signal acts as noise, reducing the ability to distinguish the weak backscattered signal from the strong interference.

To quantify this interference, the CIR is used in this project. CIR measures the strength of the backscattered signal relative to the level of interference caused by the direct link. It is defined as the ratio of the received power of the backscattered signal to that of the direct link signal. A higher CIR indicates a clearer distinction between the interference and the backscattered signal, which is crucial for accurate communication. One major difference from CLS is that the CIR implies that a certain level of the carrier (backscattered) signal is ensured.

We can express the CIR mathematically by

$$\text{CIR} = \frac{P_S}{P_I} \tag{3.22}$$

where P_S is the received power of the backscattered signal and P_I is the received power of the interfering signal from the transmitter.

Chapter 4

Results and Analysis

In this chapter, the results of the thesis are presented and analyzed. The chapter is divided into three sections. The first section outlines the evaluation metrics used, while the second explains the simulation setup. The chapter concludes with a presentation and analysis of the results, which are further categorized based on relevant comparison purposes. More specifically, Section 4.3.1 begins with observations about the impact of interference in the case of regular backscattering both in the monostatic and bistatic setups. Next, in Section 4.3.2, we present the main results of this thesis by comparing harmonic and regular backscattering and analyzing the benefits and drawbacks. We continue by explaining further studies that were conducted regarding the performance of different signal types in Section 4.3.3 and we conclude this chapter in Section 4.3.5 in which we investigate the system performance under different channel conditions.

4.1 Evaluation Metrics

To obtain the results of the thesis, we perform simulations in MATLAB on the operation of the backscattering communication system described in Chapter 3. To do so, we develop our own building blocks of the system and perform a simulation that estimates the BER of the system at the receiver for a predefined range of SNR. In this section, we explain these two fundamental metrics that are commonly used in the evaluation of communication systems and provide quantitative insights into their quality and reliability.

The first metric is BER, which is defined as the ratio of the number of bit errors to the total number of bits transmitted over a communication channel. It can be expressed by

$$\text{BER} = \frac{N_{errors}}{N_{total}} \tag{4.1}$$

where N_{errors} is the number of incorrectly received bits, and N_{total} is the total number of transmitted bits.

BER is a key performance indicator because it directly quantifies the accuracy of the data transmission. A lower BER indicates fewer errors and thus higher data reliability.

There are several factors that affect the BER.

- Noise and interference from other signals can cause bit errors.
- Low signal strength can lead to high BER.
- The choice of modulation scheme impacts the BER since different modulation schemes have different tolerances to noise and interference.
- The channel conditions, such as fading and multipath effects, also affect the BER.
- Channel coding can also help in the reduction of BER by adding redundancy to the transmitted data, allowing errors to be detected and corrected at the receiver. Note that despite its benefits, channel coding is not consider in the design of the system in this thesis.

The second metric is SNR, which fundamentally is a measure of the received signal strength to the noise level, and it is defined as the ratio of the power of the signal to the power of the noise. Usually, it is expressed in decibels (dB) as

$$\text{SNR} = 10 \log_{10} \left(\frac{P_s}{P_N} \right) \, dB \tag{4.2}$$

where P_s is the average signal power, and P_n is the average noise power.

A higher SNR indicates a clearer signal with less noise, which can generally mean better performance in BER. In essence, the SNR provides a measure of how easy the signal can be distinguished from the noise.

Some factors that affect the SNR are:

- The transmission power.
- The noise level.
- The channel quality.

- The receiver sensitivity, meaning the ability of the receiver to distinguish the signal from the noise.

There is a direct relationship between BER and SNR, commonly depicted in the form of BER vs. SNR curves. Generally, the higher the SNR, the lower the BER, meaning that the BER is a monotonically decreasing function of the SNR.

4.2 Simulation Setup

We build our simulation to fit the concept of the backscattering communication system described in Chapter 3. We consider a system that can be either monostatic or bistatic and can use either harmonic or regular backscattering. The investigated channel conditions include a simple AWGN channel, and then a Rayleigh fading and Rician fading channel with K-factor equal to 4 dB, in addition to the applied path losses. For the Rician fading channel, the value of the K factor was chosen as one of the typical ones for an indoor channel [38]. The distance between each pair of nodes is set to 20 m. For the excitation signal used by the transmitter, a single-, and multi-tone signal is simulated. It should be noted that the multi-tone signal can be seen as a simplified version of OFDM. The fundamental carrier frequency is set at 925 MHz and lies in the 5G NR FR1 n8 Downlink (DL) band. For multi-tone signal, the tones are separated by $\Delta f = 60$ kHz. The switching rate of the backscatter radio is chosen to always align with the condition of no overlap for the contiguous OFDM case, and hence calculates to 30 kHz, according to (3.19), meaning that a medium-range Analog-to-Digital Converter (ADC) is required. For the interference, in the case of monostatic regular backscattering levels of 0, 50, 60, 70, and 80 dB of CLS are simulated. In the bistatic regular backscattering case, levels of 0, 10, and 20 dB of CIR are considered. The utilized receiver is the simple baseband receiver described in Section 3.5. The defined parameters for the simulation are summarized in Table 4.1.

Since our system is subject to noise, which as explained in Chapter 2 can be modeled as a random variable, it is essential to perform Monte-Carlo simulations to accurately evaluate the performance of our system. Monte Carlo simulations are a powerful tool used to model and analyze the behavior of systems affected by randomness [39]. In our context, these simulations allow us to estimate the BER across various noise conditions and channel impairments, and for a predefined SNR range. By simulating a large number of events, we gain valuable insights into the system's performance and the impact

of different variables. The statistical nature of Monte-Carlo simulations allows us to capture complex interactions and stochastic processes that would be challenging to solve analytically. An outline of the Monte Carlo method, adjusted to our problem, can be summarized as:

1. Generate L independent realizations. L simulations are performed for each SNR value.
2. Estimate the BER for each of the L simulations.
3. Calculate the average BER for each SNR value.

One crucial point is to carefully choose L so that the desired accuracy can be achieved. In our simulation, the desired accuracy is a BER of 10^{-3}, and thus the number of simulations needed is $L = 10^4$ [39].

Table 4.1: Simulation Parameters

Setup	
Parameter	**Value**
SNR range	$(-10, 10)$ dB
Frequency band	5G NR FR1 n8, 925 MHz
Bit sequence length	100 bits
Distance	20 m
Excitation Signal Type	Single/ Multi-tone ($\Delta f = 60\,kHz$)
Channel Type	AWGN/ Rice ($K = 4\,dB$)/ Rayleigh
Setup Type	Monostatic/ Bistatic
Backscattering Type	Regular/ Harmonic
CLS	0/ 50/ 60/ 70/ 80 dB
CIR	0/ 10/ 20 dB
Number of Monte-Carlo simulations	10,000

In the next section, the results for different setup combinations are presented and analyzed.

4.3 Performance Results

4.3.1 Interference Impact

We begin by providing the results regarding the interference present in the case of regular backscattering for both monostatic and bistatic setups. We consider

the least complex setup case that assumes a single-tone excitation signal and a AWGN channel in addition to path loss.

As explained in Subsection 3.6.1, for the monostatic setup with regular backscattering, the problem of self-interference is evident in the form of carrier leakage. In this results section, we explore different levels of suppression, referred to as CLS, and assess their impact on the performance in terms of BER vs SNR. Similarly, for the bistatic setup with regular backscattering, as indicated in subsection 3.6.2, interference is present in the form of a direct-link interference between the transmitter and the receiver. Our aim is to discover the impact that different levels of CIR have on the system performance.

The results for both setups are given in Fig. 4.1.For the monostatic setup, we observe that a level of 50 dB of CLS is required for the system to have an acceptable performance, i.e., performing better than randomly guessing the received bit sequence, meaning a BER of maximum 0.1. As we increase the CLS level, the system performance is enhanced seemingly in a linear way.

In more detail, the blue curve, representing CLS = 0 dB, shows a BER that does not improve with increasing SNR, indicating that without any suppression of carrier leakage, the system cannot distinguish between signal and noise effectively. This results in a high BER, approximately equal to 0.5, regardless of the SNR. As the CLS level increases to 50 dB (orange curve), there is a noticeable improvement. However, the BER remains relatively high for lower SNR values and starts to decrease only when the SNR exceeds approximately 5 dB. Significant improvement is observed when the CLS is increased to 70 dB (purple curve) and 80 dB (green curve). The curve for CLS = 80 dB shows the best performance among all, with the BER dropping below 10^{-2} for SNR values greater than 5 dB, demonstrating that high levels of CLS are crucial for efficient backscatter communication in a monostatic setup.

Regarding the bistatic setup, setting the CIR to 0 dB (blue curve), meaning that the carrier and interference are of equal power, already demonstrates an acceptable system performance in terms of BER vs SNR. A CIR of only 20 dB is required so that the bistatic regular system has a similar performance to the monostatic regular one with a CLS of 80 dB. This indicates that the monostatic setup is more sensitive to carrier leakage and requires significant suppression to perform well, whereas the bistatic setup is inherently more resilient to interference due to the separation between the signal and interference sources.

In the following subsection, we continue by explicitly comparing harmonic and regular backscattering.

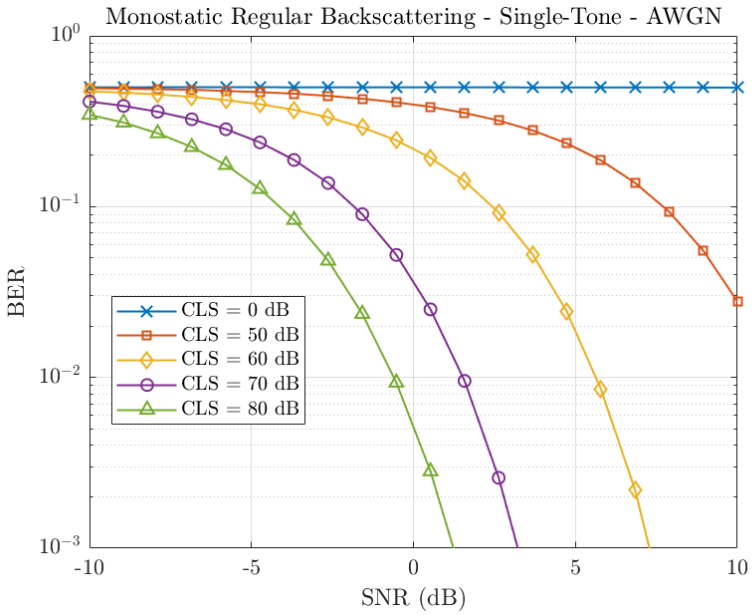

(a) CLS for monostatic setup

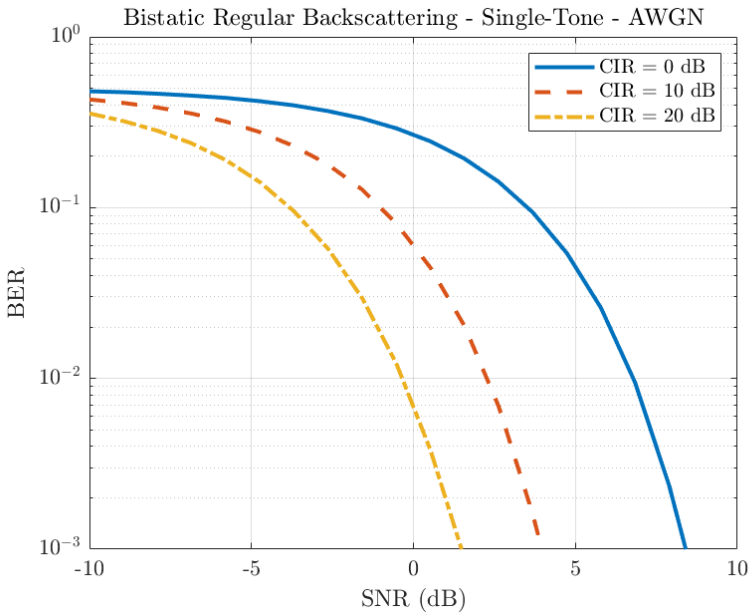

(b) CIR for bistatic setup

Figure 4.1: Interference impact in regular backscattering for the monostatic and bistatic setup simulated in an AWGN channel with a single-tone illumination signal. The BER vs SNR performance is shown for different values of CLS and CIR.

4.3.2 Harmonic vs Regular Backscattering

This subsection presents the crucial result of the thesis and is a verification of the achievement of the final goal of the thesis, stated in Section 1.4. In Fig. 4.2, we can see the performance of harmonic and regular backscattering for both monostatic and bistatic setups.

We initially chose to compare the two types of backscattering in a simple scenario where a single-tone signal is utilized as the excitation signal, and the channel is AWGN. For the monostatic setup, it is evident that harmonic backscattering (purple solid line) surpasses regular backscattering in BER vs SNR performance, with regular backscattering requiring a CLS level as high as 70 dB (yellow dash-dotted line) to outperform harmonic backscattering. This result indicates that harmonic backscattering is more beneficial since the use of complex interference suppression equipment is needed in the receiver so that the effect of self-interference can be regulated if regular backscattering is used. This requirement for high CLS levels in regular backscattering translates into more sophisticated and potentially expensive receiver designs, which can increase the overall system cost and complexity.

Similar results are witnessed in the case of the bistatic setup, in which a CIR level of 20 dB needs to be ensured so that regular backscattering can outperform the harmonic one. The reason for the difference in the values between CLS and CIR lies solely in the difference in their definition, since as mentioned in Section 3.6 the CIR implies that the carrier is guaranteed to be CIR dB higher than the interference, while the level of CLS is only the amount of interference attenuation, without any guarantee for the carrier.

In Fig. 4.3, we deliver the results for the more complex scenario of a Rician fading channel with a multi-tone signal as the excitation signal. The behavior of both setups follows the same logic as the simple case described earlier. As noticed, the performance of the system degrades in these conditions, which is something expected in multi-path fading channels. Nonetheless, harmonic backscattering continues to prevail. This can be attributed to its inherent ability to suppress interference more effectively than regular backscattering. From a practical perspective, these findings suggest that harmonic backscattering is a more reliable choice in environments with significant multi-path propagation, such as urban or indoor settings.

In the next subsection, we continue by analyzing further scenarios that were examined regarding the signal types that could potentially be utilized in the system.

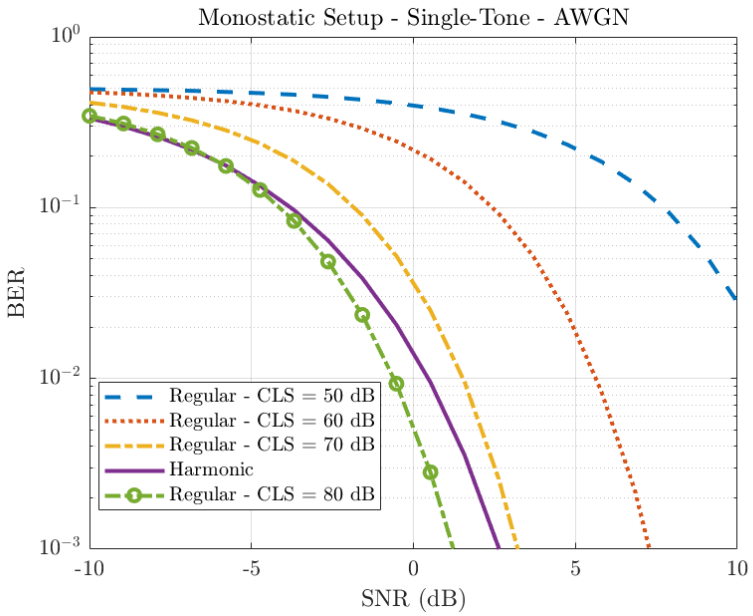

(a) Monostatic setup

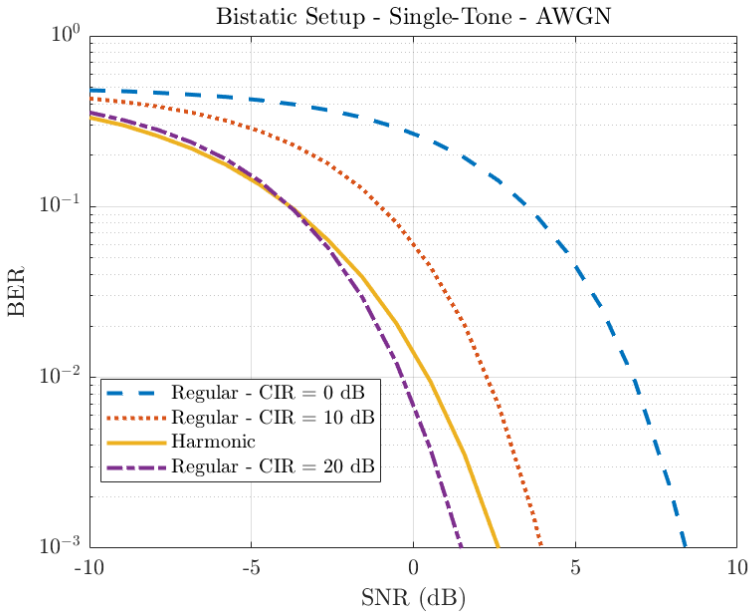

(b) Bistatic setup

Figure 4.2: Comparison of harmonic and regular backscattering with a single-tone excitation signal and AWGN channel.

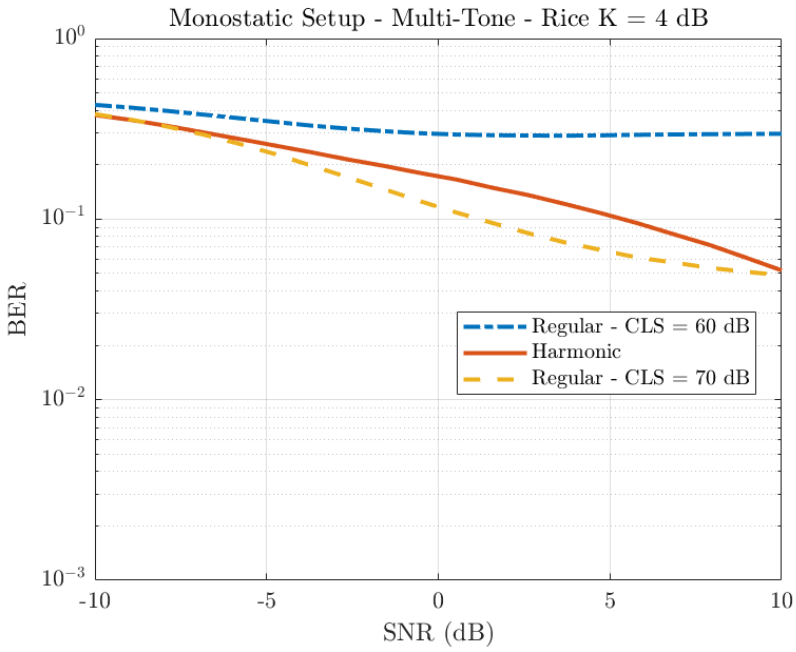

(a) Monostatic setup

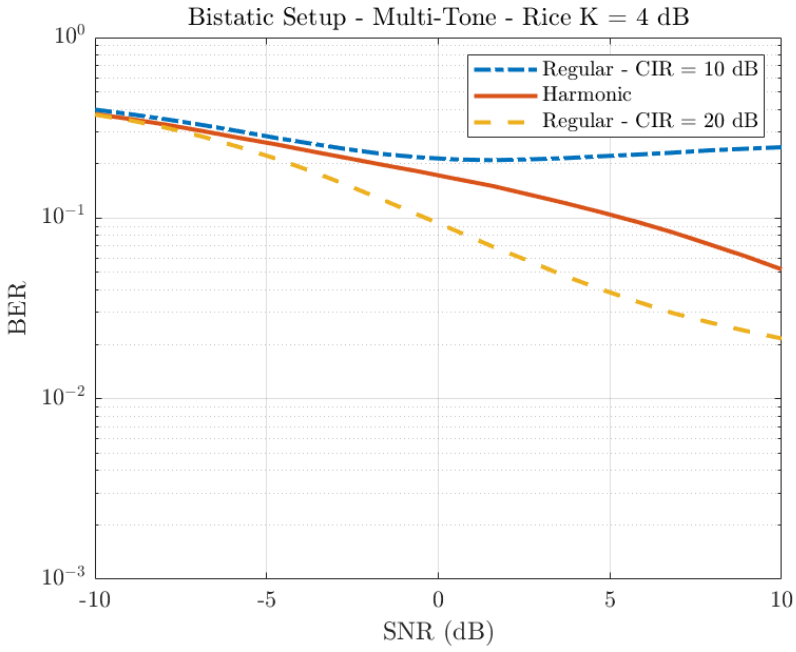

(b) Bistatic setup

Figure 4.3: Comparison of harmonic and regular backscattering with a multi-tone excitation signal and Rice channel.

4.3.3 Signal type

Having already discussed the importance of harmonic backscattering, we explore the impact of adjusting the pre-defined parameters of our system. In this section, we focus on testing various signal types that can be utilized by the transmitter. We opt to keep the comparison interest in regard to the performance of harmonic against regular backscattering to gain more perspective into the performance differences.

In Fig. 4.4, we compare different excitation signal types in the monostatic and bistatic setup, for both regular and harmonic backscattering. In the case of regular backscattering, a CLS level of 70 dB in the monostatic setup and a CIR level of 20 dB in the bistatic setup are chosen for illustration purposes. We observe that all signal types perform similarly but with some prominent differences.

In the monostatic setup, regular backscattering with a multi-tone excitation signal seems to perform slightly better than with a single-tone signal. In theory, multi-tone signals are more vulnerable to noise, and in flat-fading channels, where frequency diversity cannot be exploited, we would expect that a single-tone signal would outperform a multi-tone one. That is the case for harmonic backscattering, indicated by the blue dotted and red solid lines in the figure, where no external interference cancellation technique is utilized. Hence, we can conclude that in the regular backscattering case, the reason behind this seemingly unexpected behavior is the carrier leakage suppression that could potentially enhance the performance of the multi-tone signal by suppressing the impact of IM products caused by the non-linearities of the rectifier.

Similar behavior is observed for the bistatic setup. Regarding the difference in the performance of harmonic and regular backscattering, similar observations are evident, as in Section 4.3.2.

In the next section, we highlight the difference between monostatic and bistatic setups by performing a study on distance variation.

4.3.4 Distance variation

To further support the thesis results, and enhance the difference between monostatic and bistatic setup, we conduct simulations to evaluate the performance of the bistatic setup under varying distances between the BD and the receiver. In this scenario, the distance between the transmitter and the BD is fixed at 5 m, and the distance between the transmitter and the receiver is set at 10 m. We analyze the BER performance by varying the distance between

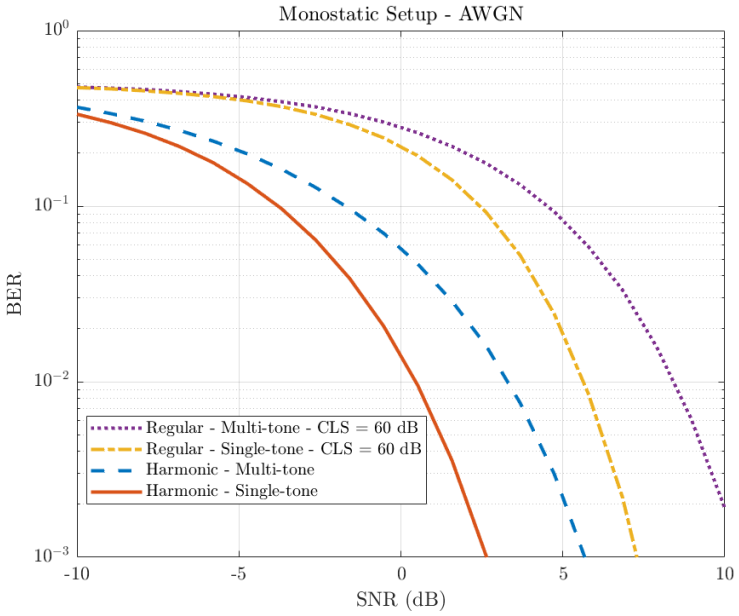

(a) Monostatic setup

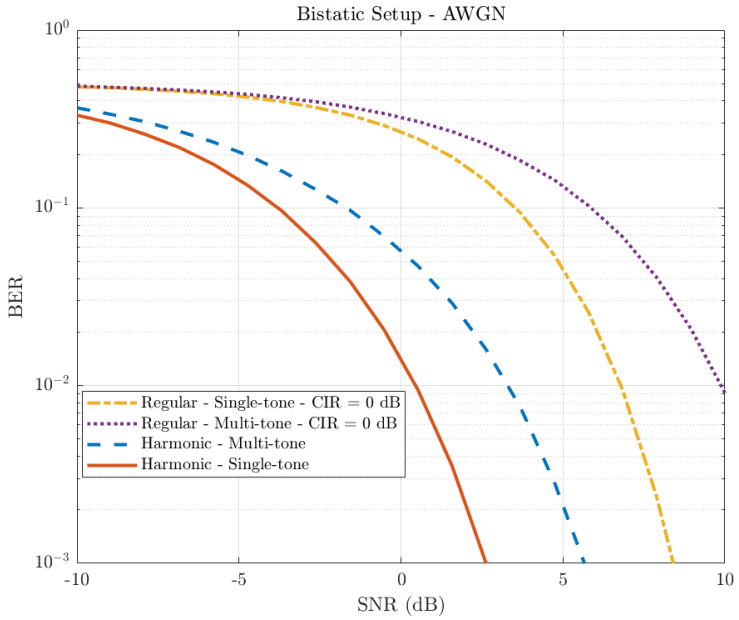

(b) Bistatic setup

Figure 4.4: Comparison between single-tone and multi-tone illumination signal in the monostatic and bistatic setup simulated in an AWGN channel.

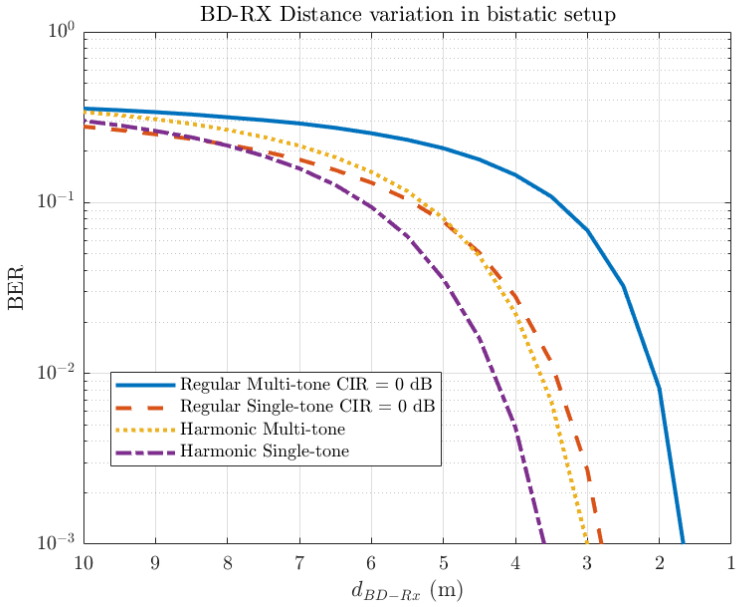

Figure 4.5: BER performance with respect to BD-Rx distance in the bistatic setup.

the BD and the receiver over a range of 1-10 m. Assuming an SNR of -5 dB at the receiver, we maintain constant noise power, using a reference estimation at 5 m. The BER at other distances is then estimated relative to the BER at 5 m. For regular backscattering, we assess performance with a CIR of 0 dB. We present the results in Fig. 4.5.

As expected, performance degrades as the distance increases. Notably, for distances beyond 8 m, regular backscattering slightly outperforms harmonic backscattering. This phenomenon can be attributed to higher path loss of the harmonic signal, due to the harmonic frequencies.

In the next section, we investigate the behavior of the system in different channel conditions.

4.3.5 Channel impact

To gain more insights into the capabilities of our backscattering system, we test under various channel conditions. In this section, we chose to focus on the monostatic setup and investigate the behavior of the system using a single-tone signal. Note that if not indicated, the chosen value of CLS for regular backscattering in monostatic setup is 70 dB and the one for CIR in bistatic setup is 20 dB.

Fig. 4.6 illustrates the BER as a function of the SNR for both harmonic and regular backscattering in a monostatic and bistatic setup, tested under three different channel conditions: AWGN, Rayleigh, and Rice with a K-factor of 4 dB. Each curve represents a specific combination of backscattering type and channel model, showing how BER decreases as SNR increases. For the monostatic setup, the data reveal that regular backscattering generally achieves lower BER than harmonic backscattering, particularly in the Rayleigh and Rice channels, where multipath effects are more pronounced. The AWGN channel results, however, show similar performance for both methods, highlighting the impact of channel characteristics on backscattering performance. The gap between the performance of harmonic and regular backscattering is more prominent under Rayleigh fading, while in Rician fading the difference is less pronounced. This observation can be supported by the fact that the presence of a line-of-sight component in the Rice channel can mitigate the negative impact of multipath fading. In general, harmonic backscattering experiences a higher BER in more complex channels, indicating its greater sensitivity to channel imperfections. This sensitivity can be attributed to the lower power of the harmonic signal. It should be highlighted that the result for regular backscattering is with the applied CLS.

Similar behavior is observed for the bistatic setup in which for regular backscattering we have the direct-link interference that is represented by the aforementioned CIR value.

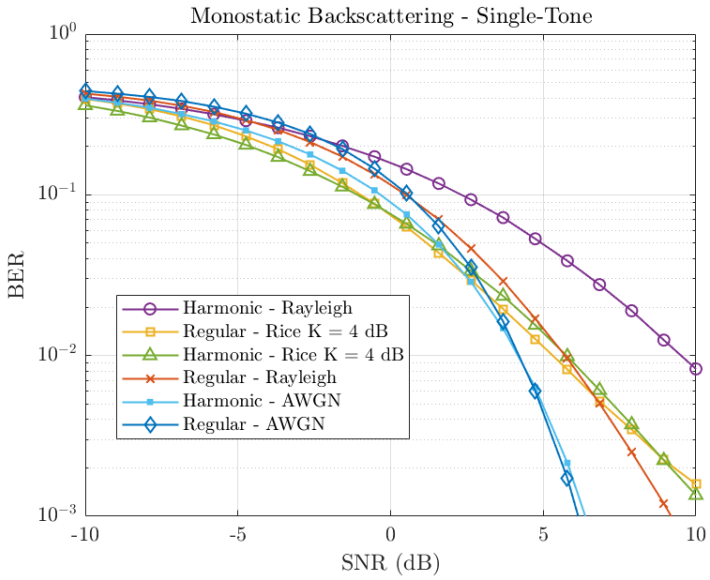

(a) Monostatic setup

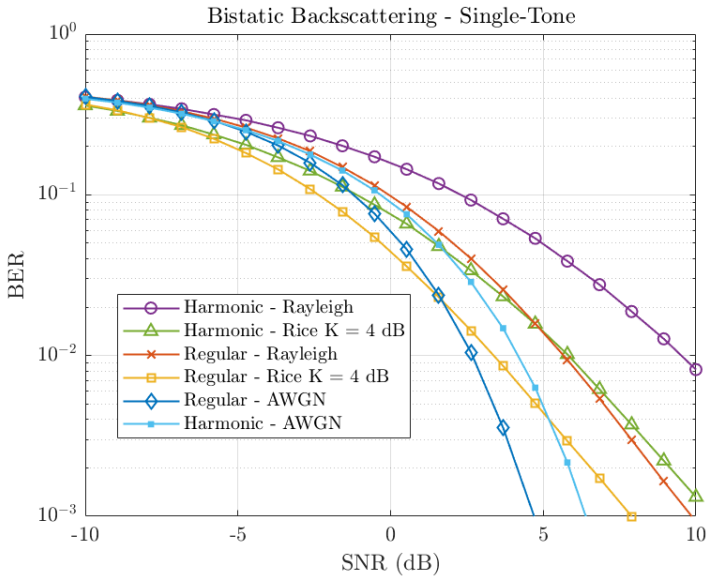

(b) Bistatic setup

Figure 4.6: Channel impact in the monostatic and bistatic setup with a single-tone excitation signal.

Chapter 5

Conclusions and Future work

This chapter provides a comprehensive overview of the findings of the research conducted on harmonic backscattering for ZEDs. In Section 5.1, we discuss the key outcomes of the study, including the positive effects of harmonic backscattering, drawbacks, and an evaluation of the results in relation to the initial goals of the project. Section 5.2 outlines the challenges and constraints encountered during the research, while Section 5.3 suggests directions for future work. Finally, in Section 5.4, personal insights and advice for future researchers in this field are shared, along with thoughts on what could be done differently if the research were to be conducted again.

5.1 Conclusions

In this thesis, we explored the potential of harmonic backscattering as a solution to the challenges faced by ZEDs in low-power communication, specifically addressing the issue of self-interference. Beginning with the mathematical modeling of the system and focusing on acquiring an expression of the generated harmonic signal at the BD, the first part of the thesis was concluded. After completing the modeling, we built a simulator to explore the performance, in terms of BER vs SNR, of harmonic backscattering in monostatic and bistatic setups, specifically against regular backscattering. The positive effects of harmonic backscattering are evident in the simulation results, which show the superiority of harmonic to regular backscattering. By shifting the backscattered signal to a harmonic frequency, the system effectively isolates the desired communication signal from the carrier, reducing interference and enabling more reliable data transmission. This performance gain is particularly pronounced in environments with high

interference, making harmonic backscattering a valuable tool for enhancing communication in IoT networks.

Through this research, several key insights were gained. First, it became clear the design of the rectifier and the modulation schemes deployed are critical to the success of this communication scheme. Variations in these parameters can have a significant impact on system performance, underscoring the need for precise control and optimization. Additionally, the study highlighted the importance of considering higher-order non-linearities in the system model, as these can influence the generation of harmonics and, consequently, the overall performance. Furthermore, the benefit of harmonic bacskcattering was highlighted both through its performance against regular backscattering and also the fact that it simplifies system design, since no interference cancellation techniques are required at the demodulator side. Another interesting observation was that for longer distances harmonic backscattering might be inferior to regular backscattering due to the higher path loss it experiences, especially when a single-tone illumination signal is used.

5.2 Limitations

Several factors limited the scope and depth of this research, impacting the outcomes. One of the primary limitations was the time constraints imposed by the duration of the project. The complexity of modeling harmonic backscattering, particularly the non-linearities introduced by the rectifier and the need to accurately simulate multiple interference scenarios, required a lot of time. This limitation constrained the variation of the scenarios explored and prevented a more exhaustive investigation of alternative system configurations.

Another significant limitation was the challenges encountered in coding and simulation. The development of the simulation model involved unexpected issues that required extensive debugging. These setbacks not only consumed valuable time but also limited the number of iterations and refinements that could be applied to the model. Consequently, the simulations, may not fully capture all real-world variances and edge cases.

Furthermore, the focus of this thesis was primarily on the physical layer of the communication system. This focus meant that higher-layer concerns, such as communication protocols, security, and channel coding were not considered. As a result, the findings are limited to the performance of the backscattering mechanism itself and do not address how these improvements might interact with or be affected by other layers of the communication stack.

This limitation is particularly relevant in real-world applications, where issues like security and protocol efficiency are critical.

Another limitation is the lack of hardware testing in this research. All findings were based on theoretical models and simulations, which do not always translate directly to practical, real-world implementations. Hardware testing could reveal practical challenges, such as power consumption issues, that were not accounted for in the simulation environment. This limitation suggests that while the results are promising, they should be validated through physical experiments before drawing definitive conclusions about their applicability in real-world scenarios.

Additionally, the results are constrained by the assumptions made during the modeling process. For example, simplified channel models and noise assumptions were used to make the problem tractable within the project's timeframe. These simplifications, while necessary, limit the generalizability of the results, particularly in environments that deviate significantly from the idealized conditions assumed in the model.

5.3 Future work

Given the scope of this project, certain areas were left unexplored, and addressing these would be the next step in this line of research.

One of the primary areas for future work is the integration of power and energy efficiency into the system model. While this thesis focused on the communication performance of harmonic backscattering, future studies should incorporate the conversion efficiency of the rectifier into the optimization problem. This would allow for a more comprehensive analysis of the trade-offs between communication reliability and energy harvesting efficiency. Moreover, developing a model that balances these factors could lead to more practical solutions for real-world applications, where both data transmission and energy efficiency are critical.

Another significant area of exploration is the investigation of alternative rectifier models. The current study employed a specific model to simulate harmonic generation and backscattering, but different rectifier designs may produce varying results in terms of efficiency and harmonic generation. Future research should consider evaluating these models, including their impact on the third-order intermodulation products, to determine the most effective design for different use cases. Additionally, incorporating higher-order non-linear terms in the mathematical expressions for the harmonics

could yield more accurate models that better reflect the complexities of real-world systems.

Expanding the study to include more advanced modulation techniques is another promising direction. While the current research focused on standard modulation schemes, experimenting with alternative techniques could further enhance the performance of harmonic backscattering systems. Towards this direction of study, one should consider the trade-off between simplicity, and hence cost, and performance, since the general trend is to keep the BD as cheap, simple, and compact as possible. This exploration could also lead to the development of new protocols that are better suited to the unique characteristics of harmonic backscattering.

Furthermore, future work should consider the application of harmonic backscattering in scenarios involving multiple devices. The current study was limited to a single-device context, but in a practical IoT environment, multiple ZEDs would likely be operating simultaneously. Investigating how these devices interact, particularly in terms of interference and network efficiency, would provide valuable insights into the scalability of harmonic backscattering systems. This research could also explore the potential for cooperative backscattering, where multiple devices work together to enhance communication coverage.

Finally, it would be beneficial to explore hardware validation early in the process. While the simulations provided a solid foundation, real-world testing could reveal practical challenges that were not apparent in the theoretical models. Additionally, considering higher-layer protocol integration, such as security measures, would be crucial for developing a complete system ready for deployment.

5.4 Reflections

From an economic perspective, the development of efficient backscattering communication techniques for ZEDs has the potential to significantly reduce the cost of network deployment. By enabling devices to operate without batteries and with minimal energy consumption, the overall maintenance and operational costs can be lowered. This reduction in costs could make IoT solutions more accessible to a broader range of industries and applications, fostering economic growth and innovation, particularly in sectors where large numbers of devices are required, such as agriculture, smart cities, and industrial automation.

Socially, the advancements presented in this thesis contribute to the

growing field of IoT, which has a profound impact on how we live and work. The ability to deploy ZEDs in remote or challenging environments, where traditional power sources are unavailable or impractical, could enhance connectivity and data gathering in areas like rural health monitoring, environmental sensing, and disaster management. This increased connectivity can lead to improved public services, better resource management, and enhanced quality of life, particularly in underserved or remote communities.

The environmental impact of this research is particularly significant. By reducing the reliance on batteries, which often contain hazardous materials and have a limited lifespan, backscattering communication supports more sustainable technology solutions. The elimination of batteries not only reduces electronic waste but also the environmental footprint associated with battery production and disposal. Additionally, the low-power nature of these devices means that they can operate using energy harvested from their surroundings, further contributing to energy conservation and sustainability goals.

Ethically, the research into backscattering communication raises important considerations regarding the security and privacy of IoT systems. As these devices become more widespread, the potential for misuse and exploitation increases. The research presented here focuses on the physical layer, but as these systems are developed further, it is crucial to incorporate security protocols to protect against unauthorized access and data breaches. Additionally, there is an ethical responsibility to ensure that these technologies do not intensify existing inequalities, particularly in terms of access to technology and information. Careful consideration must be given to how these devices are deployed and who benefits from their use.

Reflecting on the research process itself, this thesis has been a valuable learning experience, offering deep insights into the challenges associated with backscattering communication.

References

[1] "Internet of Things - Worldwide | Statista Market Forecast." [Online]. Available: https://www.statista.com/outlook/tmo/internet-of-things/worldwide [Page 1.]

[2] "State of IoT 2023: Number of connected IoT devices growing 16% to 16.7 billion globally," May 2023. [Online]. Available: https://iot-analytics.com/number-connected-iot-devices/ [Page 1.]

[3] P. Jonsson *et al.*, "Ericsson Mobility Report," Ericsson, Sweden, Tech. Rep., Nov. 2023. [Online]. Available: https://www.ericsson.com/en/reports-and-papers/mobility-report/reports/november-2023 [Page 1.]

[4] T. Khan, S. N. K. Veedu, A. Rácz, M. Afshang, A. Höglund, and J. Bergman, "Towards 6G Zero-Energy Internet of Things: Standards, Trends, and Recent Results," Preprints, preprint, Dec. 2023. [Online]. Available: https://www.techrxiv.org/users/692254/articles/693124-towards-6g-zero-energy-internet-of-things-standards-trends-and-recent-results?commit=3388a413a9563507aa46487d627d2a7d93999893 [Pages 2 and 14.]

[5] S. Naser, L. Bariah, S. Muhaidat, and E. Basar, "Zero-Energy Devices Empowered 6G Networks: Opportunities, Key Technologies, and Challenges," *IEEE Internet of Things Magazine*, vol. 6, no. 3, pp. 44–50, Sep. 2023. doi: 10.1109/IOTM.001.2200235. [Online]. Available: https://ieeexplore.ieee.org/document/10255758/ [Page 2.]

[6] C. Xu, L. Yang, and P. Zhang, "Practical Backscatter Communication Systems for Battery-Free Internet of Things: A Tutorial and Survey of Recent Research," *IEEE Signal Processing Magazine*, vol. 35, no. 5, pp. 16–27, Sep. 2018. doi: 10.1109/MSP.2018.2848361. [Online]. Available: https://ieeexplore.ieee.org/document/8454398/ [Pages 2 and 10.]

[7] W. Wu, X. Wang, A. Hawbani, L. Yuan, and W. Gong, "A survey on ambient backscatter communications: Principles, systems, applications, and challenges," *Computer Networks*, vol. 216, p. 109235, Oct. 2022. doi: 10.1016/j.comnet.2022.109235. [Online]. Available: https://linkinghub.elsevier.com/retrieve/pii/S1389128622003139 [Pages 2 and 12.]

[8] S. D. Joseph, Y. Huang, S. S. H. Hsu, A. Alieldin, and C. Song, "Second Harmonic Exploitation for High-Efficiency Wireless Power Transfer Using Duplexing Rectenna," *IEEE Transactions on Microwave Theory and Techniques*, vol. 69, no. 1, pp. 482–494, Jan. 2021. doi: 10.1109/TMTT.2020.3039604. [Online]. Available: https://ieeexplore.ieee.org/document/9290401/ [Page 3.]

[9] A. Håkansson, "Portal of Research Methods and Methodologies for Research Projects and Degree Projects." CSREA Press U.S.A, 2013, pp. 67–73. [Online]. Available: https://urn.kb.se/resolve?urn=urn:nbn:se:kth:diva-136960 [Page 5.]

[10] A. G. Bell, "The Photophone," *Science*, vol. os-1, no. 11, pp. 130–134, Sep. 1880. doi: 10.1126/science.os-1.11.130. [Online]. Available: https://www.science.org/doi/10.1126/science.os-1.11.130 [Page 9.]

[11] R. Torres, R. Correia, N. Carvalho, S. N. Daskalakis, G. Goussetis, Y. Ding, A. Georgiadis, A. Eid, J. Hester, and M. M. Tentzeris, "Backscatter Communications," *IEEE Journal of Microwaves*, vol. 1, no. 4, pp. 864–878, Oct. 2021. doi: 10.1109/JMW.2021.3110058. [Online]. Available: https://ieeexplore.ieee.org/document/9551877/ [Page 9.]

[12] H. Stockman, "Communication by Means of Reflected Power," *Proceedings of the IRE*, vol. 36, no. 10, pp. 1196–1204, Oct. 1948. doi: 10.1109/JRPROC.1948.226245. [Online]. Available: http://ieeexplore.ieee.org/document/1697527/ [Page 9.]

[13] J.-P. Niu and G. Y. Li, "An Overview on Backscatter Communications," *Journal of Communications and Information Networks*, vol. 4, no. 2, pp. 1–14, Jun. 2019. doi: 10.23919/JCIN.2019.8917868. [Online]. Available: https://ieeexplore.ieee.org/document/8917868/ [Pages 11 and 24.]

[14] N. Van Huynh, D. T. Hoang, X. Lu, D. Niyato, P. Wang, and D. I. Kim, "Ambient Backscatter Communications: A Contemporary Survey," *IEEE Communications Surveys & Tutorials*, vol. 20, no. 4, pp. 2889–2922, 2018. doi: 10.1109/COMST.2018.2841964. [Online]. Available: https://ieeexplore.ieee.org/document/8368232/ [Pages 12, 16, and 18.]

[15] Z. Ye, M. Yang, Y. Ren, C.-H. J. Hung, C.-T. M. Wu, and P.-Y. Chen, "Review on Recent Advances and Applications of Passive Harmonic RFID Systems," *IEEE Journal of Radio Frequency Identification*, vol. 7, pp. 118–133, 2023. doi: 10.1109/JRFID.2023.3276310. [Online]. Available: https://ieeexplore.ieee.org/document/10128110/ [Pages 13 and 14.]

[16] R. Weinstein, "RFID: a technical overview and its application to the enterprise," *IT Professional*, vol. 7, no. 3, pp. 27–33, May 2005. doi: 10.1109/MITP.2005.69. [Online]. Available: http://ieeexplore.ieee.org/document/1490473/ [Page 14.]

[17] W. Liu, K. Huang, X. Zhou, and S. Durrani, "Next Generation Backscatter Communication: Systems, Techniques and Applications," 2017. doi: 10.48550/ARXIV.1701.07588. [Online]. Available: https://arxiv.org/abs/1701.07588 [Page 14.]

[18] B. Sklar, *Digital communications: fundamentals and applications*, 2nd ed. Upper Saddle River, N.J.: Prentice-Hall PTR, 2001. ISBN 9780130847881 OCLC: 45823120. [Page 15.]

[19] T. S. Rappaport, *Wireless Communications: Principles and Practice*, 2nd ed. Cambridge University Press, Feb. 2024. ISBN 9781009489843 9781009489836. [Online]. Available: https://www.cambridge.org/highereducation/product/9781009489843/book [Pages 15, 20, and 21.]

[20] C. Beard and W. Stallings, *Wireless communication networks and systems*, global edition ed., ser. Always learning. Boston Columbus Hoboken Indianapolis New York San Francisco Amsterdam Cape Town Dubai London Madrid Milan Munich Paris Montreal Toronto Delhi Mexico City São Paulo Sydney Hong Kong Seoul Singapore Taipei Tokyo: Pearson, 2016. ISBN 9781292108711 [Pages 16, 17, and 18.]

[21] Q. H. Abbasi, H. T. Abbas, A. Alomainy, and M. A. Imran, *Backscattering and RF Sensing for Future Wireless Communication*,

1st ed. Wiley, Jun. 2021. ISBN 9781119695653 9781119695721. [Online]. Available: https://onlinelibrary.wiley.com/doi/book/10.1002/9781119695721 [Pages 16 and 17.]

[22] M. S. Alencar and V. C. Da Rocha, "Amplitude Modulation," in *Communication Systems*. Cham: Springer International Publishing, 2022, pp. 135–162. ISBN 9783031120664 9783031120671. [Online]. Available: https://link.springer.com/10.1007/978-3-031-12067-1_4 [Page 16.]

[23] L. Ahlin, J. Zander, and B. Slimane, *Principles of wireless communications*, andra upplagan. ed. Lund: Studentlitteratur, 2018. ISBN 9789144126531 OCLC: 1029009609. [Pages 19, 21, and 29.]

[24] J. Kimionis, A. Bletsas, and J. N. Sahalos, "Increased Range Bistatic Scatter Radio," *IEEE Transactions on Communications*, vol. 62, no. 3, pp. 1091–1104, Mar. 2014. doi: 10.1109/TCOMM.2014.020314.130559. [Online]. Available: http://ieeexplore.ieee.org/document/6742719/ [Page 24.]

[25] D. Bharadia, K. R. Joshi, M. Kotaru, and S. Katti, "BackFi: High Throughput WiFi Backscatter," in *Proceedings of the 2015 ACM Conference on Special Interest Group on Data Communication*. London United Kingdom: ACM, Aug. 2015. doi: 10.1145/2785956.2787490. ISBN 9781450335423 pp. 283–296. [Online]. Available: https://dl.acm.org/doi/10.1145/2785956.2787490 [Page 24.]

[26] J. F. Ensworth and M. S. Reynolds, "BLE-Backscatter: Ultralow-Power IoT Nodes Compatible With Bluetooth 4.0 Low Energy (BLE) Smartphones and Tablets," *IEEE Transactions on Microwave Theory and Techniques*, vol. 65, no. 9, pp. 3360–3368, Sep. 2017. doi: 10.1109/TMTT.2017.2687866. [Online]. Available: https://ieeexplore.ieee.org/document/7898833/ [Page 24.]

[27] B. Clerckx and E. Bayguzina, "Waveform Design for Wireless Power Transfer," *IEEE Transactions on Signal Processing*, vol. 64, no. 23, pp. 6313–6328, Dec. 2016. doi: 10.1109/TSP.2016.2601284. [Online]. Available: http://ieeexplore.ieee.org/document/7547357/ [Pages 25, 30, and 31.]

[28] B. A. Mouris, H. Ghauch, R. Thobaben, and B. L. G. Jonsson, "Multi-Tone Signal Optimization for Wireless Power Transfer in the

Presence of Wireless Communication Links," *IEEE Transactions on Wireless Communications*, vol. 19, no. 5, pp. 3575–3590, May 2020. doi: 10.1109/TWC.2020.2974950. [Online]. Available: https://ieeexplore.ieee.org/document/9014501/ [Page 25.]

[29] Y. Ma, Xiaonan Hui, and E. C. Kan, "Harmonic-WISP: A passive broadband harmonic RFID platform," in *2016 IEEE MTT-S International Microwave Symposium (IMS)*. San Francisco, CA: IEEE, May 2016. doi: 10.1109/MWSYM.2016.7540224. ISBN 9781509006984 pp. 1–4. [Online]. Available: http://ieeexplore.ieee.org/document/7540224/ [Page 25.]

[30] X. Chen, Y. Chen, H. Zhang, N. Yan, J. Wang, H. Min, and L. Zheng, "Long read range Class-3 UHF RFID system based on harmonic backscattering," *Electronics Letters*, vol. 54, no. 22, pp. 1262–1264, Nov. 2018. doi: 10.1049/el.2018.6007. [Online]. Available: https://onlinelibrary.wiley.com/doi/10.1049/el.2018.6007 [Page 26.]

[31] D. Kumar, S. Mondal, S. Karuppuswami, Y. Deng, and P. Chahal, "Harmonic RFID Communication Using Conventional UHF System," *IEEE Journal of Radio Frequency Identification*, vol. 3, no. 4, pp. 227–235, Dec. 2019. doi: 10.1109/JRFID.2019.2925527. [Online]. Available: https://ieeexplore.ieee.org/document/8756114/ [Page 26.]

[32] Y. Qaragoez, S. Pollin, and D. Schreurs, "Frequency Division Duplex-Multitone Approach for Backscatter Aided SWIPT," in *2022 Wireless Power Week (WPW)*. Bordeaux, France: IEEE, Jul. 2022. doi: 10.1109/WPW54272.2022.9853856. ISBN 9781665484459 pp. 213–217. [Online]. Available: https://ieeexplore.ieee.org/document/9853856/ [Page 26.]

[33] G. Yang, Y.-C. Liang, R. Zhang, and Y. Pei, "Modulation in the Air: Backscatter Communication Over Ambient OFDM Carrier," *IEEE Transactions on Communications*, vol. 66, no. 3, pp. 1219–1233, Mar. 2018. doi: 10.1109/TCOMM.2017.2772261. [Online]. Available: http://ieeexplore.ieee.org/document/8103807/ [Page 27.]

[34] M. Lopez, N. He, and T. Khan, "Designing a Bistatic Backscatter Communications System with OFDM for 6G Internet of Things," preprint, Jul. 2023. [Online]. Available: https://www.techrxiv.org/doi/full/10.36227/techrxiv.23699631.v1 [Pages 27 and 34.]

[35] D. Piumwardane, M. Padmal, V. Ranganathan, C. Rohner, and T. Voigt, "HarmonicID: An Identification System for Low-Power Analog Backscatter Tags," in *2022 IEEE International Conference on RFID (RFID)*. Las Vegas, NV, USA: IEEE, May 2022. doi: 10.1109/RFID54732.2022.9795971. ISBN 9781665410465 pp. 1–6. [Online]. Available: https://ieeexplore.ieee.org/document/9795971/ [Page 34.]

[36] A. P. Arianto, S. A. Sudiro, A. Hakim, and F. Hendajani, "Manchester encoder component for data processing IoT environment," *Journal of Physics: Conference Series*, vol. 1192, p. 012043, Mar. 2019. doi: 10.1088/1742-6596/1192/1/012043. [Online]. Available: https://iopscience.iop.org/article/10.1088/1742-6596/1192/1/012043 [Page 36.]

[37] Q. Tao, C. Zhong, H. Lin, and Z. Zhang, "Symbol Detection of Ambient Backscatter Systems With Manchester Coding," *IEEE Transactions on Wireless Communications*, vol. 17, no. 6, pp. 4028–4038, Jun. 2018. doi: 10.1109/TWC.2018.2819188. [Online]. Available: https://ieeexplore.ieee.org/document/8329444/ [Page 36.]

[38] A. De Leo, P. Russo, and V. Mariani Primiani, "Emulation of the Rician K-Factor of 5G Propagation in a Source Stirred Reverberation Chamber," *Electronics*, vol. 12, no. 1, p. 58, Dec. 2022. doi: 10.3390/electronics12010058. [Online]. Available: https://www.mdpi.com/2079-9292/12/1/58 [Page 43.]

[39] E. Björnson and . T. Demir, "Introduction to Multiple Antenna Communications and Reconfigurable Surfaces," Jan. 2024. [Online]. Available: https://nowpublishers.com/article/BookDetails/9781638283140 [Pages 43 and 44.]

TRITA – EECS-EX- 2024:949